

Receptive Fields and Functional Architecture of Macaque V2

JONATHAN B. LEVITT, DANIEL C. KIPER, AND J. ANTHONY MOVSHON

Howard Hughes Medical Institute, Center for Neural Science, and Department of Psychology, New York University, New York, New York 10003

SUMMARY AND CONCLUSIONS

1. Visual area V2 of macaque monkey cerebral cortex is the largest of the extrastriate visual areas, yet surprisingly little is known of its neuronal properties. We have made a quantitative analysis of V2 receptive field properties. Our set of measurements was chosen to distinguish neuronal responses reflecting parvocellular (P) or magnocellular (M) inputs and to permit comparison with similar measurements made in other visual areas; we further describe the relationship of those properties to the laminar and cytochrome oxidase (CO) architecture of V2.

2. We recorded the activity of single units representing the central 5° in all laminae and CO divisions of V2 in anesthetized, paralyzed macaque monkeys. We studied responses to geometric targets and to drifting sinusoidal gratings that varied in orientation, spatial frequency, drift rate, contrast, and color.

3. The orientation selectivity and spatial and temporal tuning of V2 neurons differed little from those in V1. As in V1, spatial and temporal tuning in V2 appeared separable, and we identified a population of simple cells (more common within the central 3°) similar to those found in V1. Contrast sensitivity of V2 neurons was greater on average than in V1, perhaps reflecting the summation of inputs in V2's larger receptive fields. Many V2 neurons exhibited some degree of chromatic opponency, responding to isoluminant color variations, but these neurons differed from V1 in the linearity with which they summate cone signals.

4. In agreement with others, we found that neurons with selective responses to color, size, and motion did seem to cluster in different CO compartments. However, this segregation of qualitatively different response selectivities was not absolute, and response properties also seemed to depend on laminar position within each compartment. As others also have noted, we found that CO stripe widths in the macaque (unlike in the squirrel monkey) did not consistently appear different. We relied on the segregation of qualitatively distinct cell types, and in some cases the pattern of Cat-301 staining as well, to distinguish CO stripes when the staining pattern of CO alone was ambiguous. Although all cell types were found in all CO compartments and laminae, unoriented cells were more prominent in layers 2–4 of “thin” stripes, direction-selective cells in layers 3B/4 of “thick” stripes, color-selective cells in the upper layers of thin and pale stripes, and end-stopped cells mainly outside of layer 4 in thin stripes.

5. Cells in the different CO compartments differed little in their spatial, temporal, and contrast sensitivity or in their orientation selectivity, although thin-stripe cells more commonly were unoriented and had somewhat lower spatial resolution and contrast sensitivity than did cells in thick and pale stripes. Thus whereas our results are broadly consistent with functional segregation across V2, they also suggest that the physiological organization of V2 is substantially more homogeneous than has been previously appreciated and are inconsistent with continued segregation of P and M signals in V2.

INTRODUCTION

Primate cerebral cortex contains some functionally distinct visual areas outside the primary visual cortex (for reviews, see Felleman and Van Essen 1991; Maunsell and Newsome 1987). Evidence suggests that these visual cortical areas are arranged into two parallel functional streams that analyze distinct types of visual information (DeYoe and Van Essen 1988; Maunsell and Newsome 1987; Ungerleider and Mishkin 1982; Van Essen and Maunsell 1983). The root of both streams is in primary visual cortex (V1) and the adjacent prestriate area V2. From these, a ventral pathway projects via area V4 to the visual cortex of the inferior temporal lobe and seems to be concerned with aspects of form and color vision. A dorsal pathway projects via areas V3 and MT to the visual cortex of the posterior parietal lobe and seems involved in visual motion analysis, the direction of attention, and other visuomotor functions.

Regions in V1 and V2 defined by cytochrome oxidase (CO) staining have distinct anatomic connections and physiological properties that seem to tag these regions as belonging to one of the two functional streams through visual cortex. The superficial V1 layers contain patches of tissue (now known as “blobs” or “puffs”) rich in CO (Horton and Hubel 1981; Humphrey and Hendrickson 1983). V2 also contains regions of high- and low-CO activity arranged into alternating thick and thin stripes of CO-rich tissue separated by CO-sparse pale-stripe regions. Cells in the V1 blobs project to the thin stripes in V2, whereas cells in the V1 interblob regions project to the V2 pale stripes (Livingstone and Hubel 1984). The V2 thin stripes contain many nonoriented, color-selective cells whereas the pale-stripe regions contain many orientation-tuned cells (Hubel and Livingstone 1987). Cells in both the thin and the pale stripes project to V4 (DeYoe and Van Essen 1985; Shipp and Zeki 1985; Zeki and Shipp 1989), an action that is consistent with the notion that these regions are part of a pathway for color and form analysis. A different set of anatomic connections distinguishes the motion pathway. V1 neurons in layer 4b project to MT (Lund et al. 1981; Movshon and Newsome 1984; Shipp and Zeki 1989a) and to the V2 thick stripes (Livingstone and Hubel 1987), which contain direction-selective cells and are known to project to area MT themselves (DeYoe and Van Essen 1985; Shipp and Zeki 1985, 1989b).

Neuronal responses differ between the two pathways. For example, neurons in MT are sensitive to motion and binocular disparity but rarely to color (Dubner and Zeki 1971; Maunsell and Van Essen 1983a,b; Zeki 1974), whereas neurons in V4 and IT are highly sensitive to the shape or color

of stimuli and rarely to the direction of stimulus motion (Desimone and Schein 1987; Desimone et al. 1985; Schein and Desimone 1990; Zeki 1978). These differences have led to characterization of the pathways for object versus spatial vision (Ungerleider and Mishkin 1982) or for motion versus color and form (Van Essen and Maunsell 1983). There has been much interest recently in determining more precisely how neuronal response properties differ between the two pathways and the extent to which the different extrastriate visual areas (and the visual functions they subserve) derive their primary excitatory drive from signals relayed through either the parvocellular (P) or magnocellular (M) divisions of the lateral geniculate nucleus (LGN) (Livingstone and Hubel 1988; Maunsell et al. 1990; Schiller et al. 1990).

Because cells in the M and P divisions of the LGN have different physiological properties (Derrington and Lennie 1984; Derrington et al. 1984; Dreher et al. 1976; Hicks et al. 1983; Kaplan and Shapley 1982; Schiller and Malpeli 1978; Sherman et al. 1984; Wiesel and Hubel 1966) and segregated inputs to layer 4 of V1 (Hendrickson et al. 1978; Hubel and Wiesel 1972), it has been suggested that the differences between the two visual pathways reflect the relative dominance of P or M signals (Livingstone and Hubel 1988). Consistent with this suggestion, Maunsell et al. (1990) demonstrated that responses in area MT depended on M input. Recent anatomic studies have demonstrated, however, that there is substantial convergence of P and M signals in the upper layers of V1 (Lachica et al. 1992; Yoshioka et al. 1994), and this convergence can be detected physiologically (Nealey et al. 1991). Despite the widespread interest in determining the extent to which P and M signals remain segregated through visual cortex and the anatomic evidence that many V1 neurons have access to both signals, few measurements of neuronal responses have been reported that might distinguish these signals in other visual areas. Visual area V2 seemed a promising place to examine functional differences between the two pathways, as well as P/M segregation. V2 is the first area in the visual pathway having extensive connections to both parietal and temporal visual areas and is a region where different types of information seem to be segregated before being relayed to other cortical areas. As noted above, inputs to the different CO compartments in V2 arise from distinct subregions of V1. Is there a strict segregation of physiological properties matching the segregation of cortical connections? Because different types of visual information are relayed through adjacent parallel strips of tissue in V2, interactions between different pathways might occur. Indeed, descriptions already exist of laterally spreading intrinsic connections within V2 (Levitt et al. 1994; Lund et al. 1981; Rockland 1985).

V2 is the largest of all the visual cortical areas save V1 and provides a major output to the other extrastriate visual areas, yet surprisingly little is known about its receptive field properties. Previous studies of V2 physiological characteristics have been qualitative for the most part (Baizer et al. 1977; DeYoe and Van Essen 1985; Gattass et al. 1981; Hubel and Livingstone 1985, 1987). Those studies essentially were limited to determining the existence of qualitatively distinct cell groups, such as directionally selective or nonoriented cells, and the distribution of these cells relative

to anatomic landmarks in V2 such as the CO stripes. Conversely, those studies that attempted to measure neuronal responses in more detail (Burkhalter and Van Essen 1986; Foster et al. 1985; Orban et al. 1986) did not effectively compare the properties of the cell types others had recognized or relate these properties to the anatomic structure of V2.

In this paper, we describe a quantitative analysis of V2 receptive field properties and the relationship of those properties to the laminar and CO architecture of V2. Our measurements were chosen to distinguish neurons bearing the response signatures of P or M input, and to permit comparison with similar measurements made in other visual areas. Our results suggest that in many respects neuronal responses in V2 do not differ greatly from those in V1. Furthermore the segregation of neurons with distinctive properties is not absolute and neuronal responses in different CO compartments are generally similar to one another, inconsistent with segregation of P and M signals through V2.

Some of these results have been described briefly elsewhere (Levitt et al. 1990).

METHODS

Preparation and maintenance

These experiments, 3–4 days in duration, were performed on 13 young adult *Macaca fascicularis* monkeys weighing between 3 and 4 kg. Animals were premedicated initially with atropine (0.25 mg), and acepromazine (0.05 mg/kg) or diazepam (Valium, 0.5 mg/kg). After induction of anesthesia with intramuscular injections of ketamine HCl (Vetalar, 10–30 mg/kg), cannulae were inserted in the saphenous veins and surgery was continued under intravenous anesthesia. In the early experiments, we used sodium thiopental (Pentothal, 1–2 mg·kg⁻¹·hr⁻¹) for anesthesia. In most experiments, the opiate anesthetic sufentanil citrate was used for both surgery and maintenance (Sufenta: 4–8 µg·kg⁻¹·hr⁻¹). Neurons in animals anesthetized with sufentanil citrate seemed to give more vigorous responses than those from barbiturate-anesthetized animals. However, we found no difference in the pattern or selectivity of neural responses.

After cannulation of the trachea, the animal's head was fixed in a stereotaxic frame. A small craniotomy was made over the lunate sulcus, and after making a small slit in the dura, a tungsten-in-glass microelectrode (Merrill and Ainsworth 1972) was positioned just behind the lunate sulcus lip near the representation of the fovea in V2; the hole was covered with warm agar. Electrode penetrations were directed down the posterior bank of the lunate sulcus, at an angle ≤5 degrees from vertical. This permitted the study of receptive fields from the representation of the central 5° of V2. Action potentials were amplified and displayed conventionally; standard pulses triggered by each impulse were stored by a PDP11 computer and also were fed to an audiometer.

After surgery, animals were paralyzed to minimize eye movements. Paralysis was maintained with an infusion of pancuronium bromide (Pavulon, 0.1 mg·kg⁻¹·hr⁻¹) or vecuronium bromide (Norcuron, 0.1 mg·kg⁻¹·hr⁻¹) in lactated Ringer solution with dextrose (5.4 ml/hr). Animals were ventilated artificially with room air or a 49:49:2 mixture of N₂O, O₂, and CO₂. Peak expired CO₂ was maintained at 4.0% by adjusting the respirator stroke volume or the CO₂ content in the gas mixture. Rectal temperature was kept near 37°C with a thermostatically controlled heating pad. Anesthesia was maintained by continuous infusion of sodium pentobarbital (Nembutal, 1–2 mg·kg⁻¹·hr⁻¹) or sufentanil citrate (Sufenta, 4–8 µg·kg⁻¹·hr⁻¹). The EKG, electroencephalogram,

lograph, and rectal temperature were monitored continuously to ensure the adequacy of anesthesia and the soundness of the animal's physiological condition. Animals also received daily injections of a broad-spectrum antibiotic (Bicillin, 300,000 units) as well as dexamethasone (Decadron, 0.5 mg/kg) to prevent cerebral edema.

The pupils were dilated and accommodation paralyzed with topical atropine, and the corneas were protected with zero power contact lenses; supplementary lenses were chosen that permitted the best spatial resolution of recorded units. Lenses were removed periodically for cleaning and the eyes rinsed with saline. The lenses also were removed for several hours each day, the eyes given a few drops of ophthalmic antibiotic solution (Gentamicin), and the lids closed. Before beginning each day's recording, the foveas were located and plotted using a reversible ophthalmoscope.

Track reconstruction and histology

During recording, small electrolytic lesions were produced at locations of interest along the electrode track by passing DC current (1–2 μ amps for 2–5 s, tip negative) through the electrode tip. At the end of the experiment, the animals were killed with an overdose of Nembutal and perfused through the heart with 0.1 M phosphate-buffered saline (PBS, 2 l), followed by a solution containing 4% paraformaldehyde in 0.1 M PBS (2 l; the first liter also contained 4% sucrose, the second liter also had 12% sucrose). Blocks containing the region of interest were stored overnight in the cold in a postfix solution of 4% paraformaldehyde plus 30% sucrose, after which 40- μ m-thick coronal sections were cut on a freezing microtome. Alternate sections were stained for Nissl substance with cresyl violet or cytochrome oxidase by Silverman and Tootell's (1987) modification of the method of Wong-Riley (1979). In four hemispheres, to aid in stripe identification, we stained alternate tissue sections (or counterstained CO sections) for Cat-301 immunoreactivity using the protocol described by DeYoe et al. (1990).

In this study, we reconstructed recording penetrations from coronally sectioned tissue. In coronal sections, it can be difficult to distinguish thick and thin stripes on the basis of appearance alone. Cytochrome oxidase staining in macaque V2 can be quite irregular; bifurcations or inhomogeneities within each stripe region are common, unlike squirrel monkey V2 in which the stripes are distinguished much more easily. Because the pattern of alternating stripes was usually ambiguous in single sections, we also relied on serial reconstructions of CO-stained material to identify stripe boundaries. Despite these difficulties, we avoided flattening cortex and cutting tangentially and elected to section coronally to permit better laminar localization of recording sites. However, we were still left with the problem of stripe identification. It became clear during these experiments that qualitatively different properties did indeed cluster in alternate dark stripes. One set of dark stripes was found to contain clusters of unoriented and/or color-selective cells, whereas the other set contained clusters of directional cells. Following previous work in both squirrel and macaque monkey, we have called those stripes containing clusters of unoriented and color cells "thin" and those stripes containing clusters of directional cells "thick" (Hubel and Livingstone 1987). To obtain a more objective marker of stripe identity, we also in several cases reacted tissue sections containing electrode tracks for Cat-301 immunoreactivity; the Cat-301 antibody has been shown to label preferentially the thick stripes (DeYoe et al. 1990; Hendry et al. 1988). In those cases where CO-stained material was counterstained for Cat-301, although the absolute number of labeled cells was somewhat lower than in fresh tissue, we could still distinguish Cat-301 labeling from CO. Cat-301 label was characteristically somewhat granular and limited to the cell membrane surrounding the soma and proximal dendrites, whereas CO staining was more

uniform, limited to the soma, and lacked the distinctive granular membrane pattern. We found perfect agreement between our stripe identification and the Cat-301 labeling in the cases in which this label was used.

Visual stimulation

Achromatic stimuli were presented within a circular mask on the face of a display oscilloscope (1332A, Hewlett-Packard) with a P31 phosphor and a mean luminance of 40 cd/m². At the viewing distance of 57 cm, the screen subtended 9.5° at the monkey's eye. Stimulus presentation was controlled by a PDP11 computer, which also accumulated, stored, and analyzed neuronal response data. In some experiments, chromatic as well as achromatic stimuli were produced on the face of a color monitor (7211C13, Conrac) driven by signals from a display processor (3006, Adage). In these experiments, the monitor was placed 228 cm from the animal, at which distance the screen subtended 6.75° × 7.25°. Stimuli generally were confined to a central 5°-square region in the center of the screen, although they could be made larger or windowed for units with inhibitory surround or end regions. This central region was surrounded by a uniform white field with the same mean luminance as our stimuli. The display refresh rate was 120 Hz interlaced. The mean luminance of the monitor was 70 cd/m². Nonlinearities in the relation between applied voltage and phosphor luminance were compensated for by appropriate nonlinearities in the three-color lookup tables.

To describe the chromatic stimuli, we used a color space of Derrington et al. (1984). In this space, all stimuli are defined as spatiotemporal modulations about a white point of average chromaticity and luminance. Along one axis of this space—the red-green (RG) axis—stimulus modulation causes no change in the excitation of the short-wavelength-sensitive (S) cones; the excitations of the long (L)- and middle (M)-wavelength-sensitive cones covary so as to keep their sum constant. Along the blue-yellow (BY) axis, stimulus modulation causes no change in the excitations of the R and G cones; only B cone excitation changes. These two axes define a plane, the isoluminant plane, in which only chromaticity varies. The intersection point of these axes defines the white point. The CIE chromaticity coordinates of our white point were 0.336, 0.350; the coordinates are close to an equal energy white. Orthogonal to the isoluminant plane, and also passing through the white point, is a third axis, the achromatic axis. Along this axis, the luminance of stimuli changes; the excitation of all three cone types varies proportionally. A vector in this color space is defined by two parameters: its azimuth (ϕ) with respect to the RG axis and its elevation (θ) with respect to the isoluminant plane. ϕ can take values between 0 and 360°, and θ can take values between -90 and 90°. Stimuli in these experiments were either spatially uniform fields whose chromaticity and luminance were modulated in time along a vector through the white point, or sinusoidal gratings similarly modulated in space. Note that the scaling of the axes in this space is not absolutely defined, but is determined by the characteristics of the display in use. Modulations that do not lie along one of the cardinal axes are arbitrary and cannot simply be compared with measurements made in other laboratories. We defined unit modulation along any axis to be 70% of the maximum obtainable and chose modulations of equal depth in all directions in color space. In terms of the modulation of signals of each individual cone class, the maximum modulations were 0.18 for the L cones, 0.09 for the M cones, and 0.90 for the S cones.

Characterization of receptive fields

Receptive fields were mapped initially by hand on a tangent screen using black-and-white or colored geometric targets. When a single neuron's activity was isolated, we established the neuron's

dominant eye and occluded the other for quantitative experiments. Because almost all V2 neurons are equally well driven by the two eyes, the choice of eye was generally not critical. A few neurons, unresponsive to monocular stimulation, responded to required binocular stimulation, but such obligate-binocular cells were rare. We first mapped the location and size of the neuron's minimum response field and then determined selectivity for the orientation, direction of motion, color, or size (particularly end stopping) of stimuli. We used four broad-band gelatin (Wratten) filters (red, green, blue, yellow) for our initial determination of color selectivity. We classified cells as color-selective if their responses were clearly better to one color of target (other than white) or if they gave frankly opponent responses. When assessing color selectivity in this way, we tested each color over a range of luminances to be certain that response differences could not be attributed to brightness differences. Cells whose responses diminished as bar or slit length was increased were classified as end stopped. After this initial qualitative characterization, we positioned the receptive field on the face of a display CRT, and quantitative experiments using sinusoidal grating stimuli proceeded under computer control.

Each experiment consisted of several (generally 4–10) blocks of trials. Within each block, all stimuli were presented for the same amount of time (generally 5–10 s). Using these stimulus durations, we observed no consistent habituation of responses relevant to the interpretation of results. To minimize effects of response variability, stimuli were presented in a random order within each experimental block, and the results of several repeated blocks averaged. Responses were compiled into average histograms synchronized to each temporal cycle of the stimulus. These histograms were then Fourier analyzed to calculate responses at DC and at the fundamental stimulus frequency (F1). For complex cells, which respond with an unmodulated elevation in discharge rate, we used the DC response (mean firing rate minus spontaneous activity) as the response measure; for simple cells we used the F1 response. We also measured responses to a uniform field of the same mean luminance as our grating stimuli to measure the cell's spontaneous firing rate. Except for the measurement of contrast response functions, contrast was generally held constant at 0.5 or 0.7 within a single stimulus block.

RESULTS

We studied 213 single units in V2, in 20 penetrations from 13 hemispheres. Receptive fields were mainly in the central 5°, although we did occasionally sample as far peripheral as 9°. After mapping their receptive fields, 44 cells were lost; of the remainder, 20 cells (12%) were unresponsive to gratings, and 149 cells (88%) were recorded long enough to obtain quantitative response data.

Description of measurements

ORIENTATION. Figure 1 illustrates the kinds of measurements made for each cell encountered in V2. All response plots shown in Fig. 1 are from the same cell. Using gratings of the estimated optimal spatial frequency and drift rate, we first measured orientation selectivity (Fig. 1A). In this and subsequent figures, spontaneous activity has been subtracted from DC responses. This direction-selective cell responded best to vertical gratings drifting to the right. We fit regression lines to the orientation-response curve on both sides of the peak response point, and from this fit determined half the difference in degrees between the two orientations where response had fallen to half the maximum (the halfwidth). Cells with responses that had fallen to baseline

at an orientation near that orthogonal to the peak (such as those in Fig. 1A) were called orientation selective. Cells with responses that fell to less than half the peak at a near orthogonal orientation, but never fell to baseline were called orientation biased, and cells with responses that never fell below half the peak value were classified as nonoriented.

SPATIAL FREQUENCY. Using gratings of the optimal orientation and estimated optimal drift rate, we then measured responses to drifting gratings whose spatial frequency varied in half-octave steps from 0.1 to 10 or more cycles/degree. We also measured responses to full-field modulation (0 cycles/°). To each spatial-frequency response function, we fit a difference-of-exponentials function from which we derived the optimal spatial frequency, the spatial-frequency bandwidth, and the spatial resolution. *Spatial-frequency bandwidth* is the ratio between the high and low spatial frequencies where response has fallen to half the maximum response, in octaves. In some cases, the spatial-frequency response curve had little or no rolloff at low spatial frequencies and a bandwidth measure could not be obtained for such cells. Some of these cells genuinely responded best to gratings of 0 cycles/°, but others instead had response curves that were flat out to some spatial frequency and then dropped. For these cells, we chose as the "optimal" spatial frequency not 0 cycles/°, but the corner spatial frequency at which responses began to fall. *Spatial resolution* is the highest spatial frequency to which the cell reliably responds. We devised a statistical analysis of responses on the basis of the contrast response function to determine the response level that was just reliably above baseline (see below). For those cells for which we were unable to perform this statistical analysis, we chose the spatial frequency at which response had fallen to 15% of the peak, as this was found to be the average for those cells for which a statistical analysis was performed. Figure 1B shows results from such an experiment. The solid curve is the best-fitting difference-of-exponentials function, and the arrow indicates the spatial resolution of the cell.

TEMPORAL FREQUENCY. We next measured the response to drifting gratings of different temporal frequencies at the optimal orientation and spatial frequency. To the temporal frequency-response data, we fit a function representing cascaded low-pass exponential and high-pass RC filters and determined the optimal temporal frequency, temporal resolution, and temporal-frequency bandwidth (defined as for spatial frequency above). Several V2 cells did not have band-pass temporal-frequency characteristics. We could not calculate a bandwidth for these low-pass cells. As for the spatial-frequency data, if a cell's temporal-frequency tuning curve was flat out to some value, we chose as optimal the frequency at which responses began to drop. Figure 1C illustrates results from such an experiment. The solid curve here represents the best-fitting curve, and the arrow indicates the temporal resolution of the cell.

CONTRAST. We used gratings of the optimal orientation, spatial frequency, and drift rate to measure the cell's sensitivity to contrast. Figure 1D shows typical contrast-response data. We varied contrast in steps of $\sqrt{2}$ from 0.016 up to 0.50. In later experiments using the Adage display, we

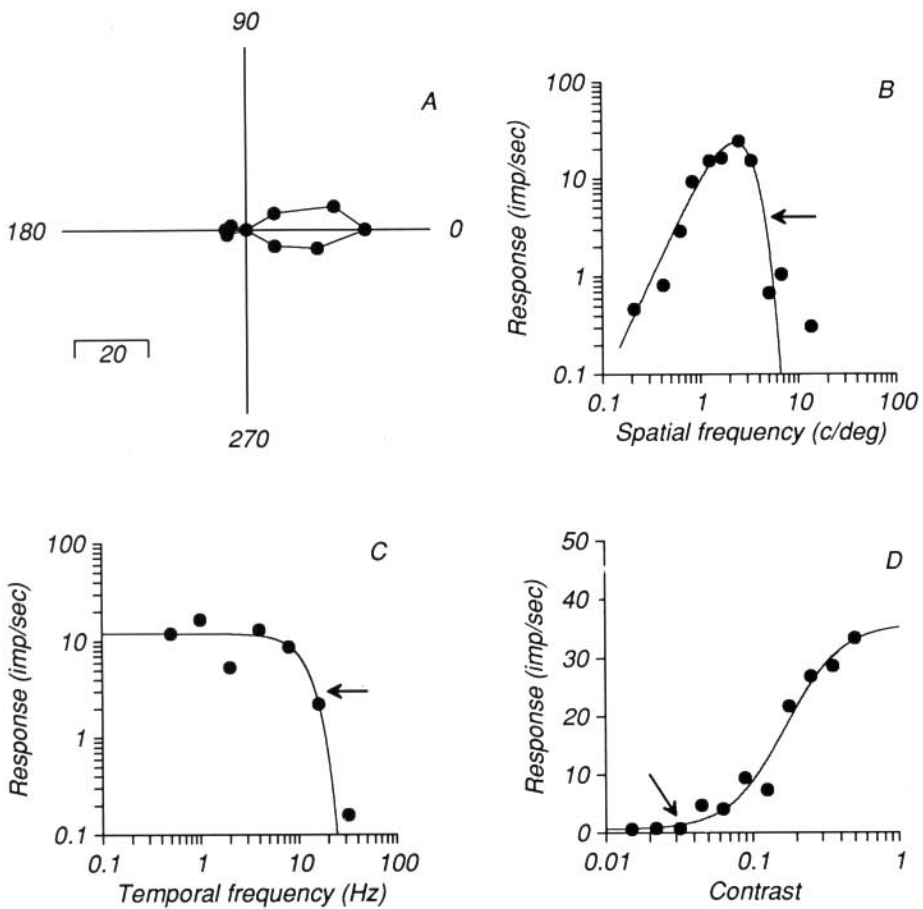


FIG. 1. Representative response measures. This direction-selective cell was located in layer 4 of a thick cytochrome oxidase (CO) stripe. *A*: angular position represents grating stimulus' orientation and distance from the origin represents response magnitude. Zero degrees represents a vertical grating drifting to the right, whereas 90° represents a horizontal grating drifting up. *B*: solid line is the best-fitting difference-of-exponentials function and arrow indicates the spatial resolution of the cell. *C*: solid line is the best-fitting temporal tuning function and arrow indicates the temporal resolution of the cell. *D*: solid line represents best-fitting hyperbolic function and arrow indicates the threshold contrast level. (See text for explanation of derived parameters.)

were able to vary contrast ≤ 0.95 . To contrast-response data, we fitted the hyperbolic function used by Albrecht and Hamilton (1982), who have shown that this function accurately describes contrast-response data from striate cortex. We extracted two parameters from this function to describe the contrast-response properties of V2 neurons: the semisaturation constant, the contrast at which the function reached half maximum, and the exponent, which describes the function's steepness. The solid curve in Fig. 1*D* is the best-fitting contrast-response function for this cell.

We performed the statistical analysis introduced by Tolhurst et al. (1983) of the responses of each neuron to determine the threshold contrast for each neuron, i.e., the contrast level at which responses were just distinguishable from the maintained discharge of the cell. We defined threshold as the contrast at which the neuron would correctly signal the presence of a grating 57% of the time (Fig. 1*D*, →). This value was chosen as the binomial probability level 1 standard deviation above chance performance. Contrast sensitivity is the reciprocal of this contrast.

CHROMATIC PROPERTIES. We measured the chromatic properties of V2 neurons using optimal gratings and uniform fields. To sample color space efficiently, the stimuli were modulations spaced 45° apart in each principal plane. Figure 2 illustrates the responses of two V2 neurons to the complete set of stimuli, in each case using gratings of the cell's optimal spatial frequency. Derrington et al. (1984) and Lennie et al. (1990) previously have utilized these stim-

uli to investigate the chromatic properties of neurons in macaque LGN and striate cortex. If a neuron sums cone inputs linearly, then its response in any direction in color space should simply be the projection of that stimulus onto the direction of best response. This describes a sinusoidal modulation of response in each of the three principal planes of color space. We found it necessary, however, to fit our data with sinusoids modified to include offset and exponent terms (to account for responses that were more or less narrowly tuned and that did not fall to zero). To describe the chromatic properties of each cell, we extracted from the fits the optimal azimuth (ϕ_m) and elevation (θ_m), i.e., the direction in color space in which the cell would respond best. The solid lines through the data in Fig. 2 represent the best-fitting sinusoids.

Each panel of Fig. 2 plots responses in different directions through each principal plane. Figure 2, *A–C*, shows data from one typical V2 cell. This cell was only poorly responsive to purely chromatic modulation in the isoluminant plane, but responded quite well to all modulations out of the isoluminant plane. This cell responded best to stimuli that were elevated close to 90° out of the isoluminant plane, i.e., to purely luminance variations. The solid lines through the data points are the best-fitting modified sinusoids, and the fit yielded ϕ_m and θ_m values of 5° and 78°. These data were reasonably well described by the fits, and resembled most V1 neurons in that respect (Lennie et al. 1990).

We also found cells that were responsive to isoluminant color modulations. Figure 2, *D–F*, plots data from one

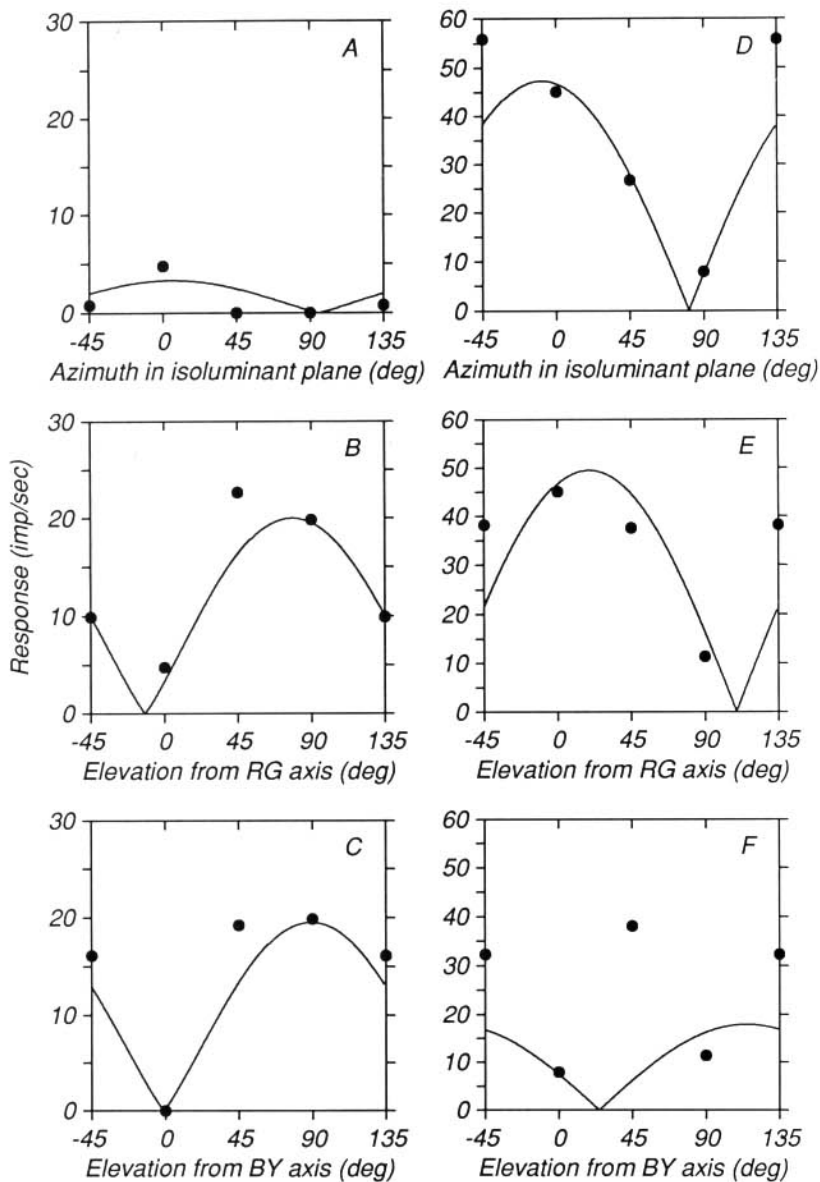


FIG. 2. Representative chromatic measurements. Responses were measured to chromatic modulations spaced 45° apart in each of the 3 principal planes of color space (the isoluminant plane, the plane defined by the intersection of the RG and luminance axes, and the plane defined by the intersection of the BY and luminance axes). Solid lines through data points are best-fitting (modified) sinusoids. A-C: illustrated responses of an oriented complex cell in layer 6. This cell's optimal elevation (θ_m) and optimal azimuth (ϕ_m) were 78° and 5°, respectively. Note weak responses in the isoluminant plane and robust responses to stimuli with elevations near 90° (pure luminance stimuli). D-F: illustrated responses of oriented simple cell in layer 3 (ϕ_m and θ_m were -9° and 19°). This cell responded much more strongly to isoluminant color variations than did the other cell, but it also responded well to luminance variations.

such cell. This cell responded well to modulations within the isoluminant plane, but was also responsive in each of the two other planes of color space. ϕ_m and θ_m for this cell were -9° and 19°. The data for this neuron were not so well described by the modified sinusoids; the departures from linear combination of cone signals implied by this kind of failure have been explored in further experiments in this laboratory (Gegenfurtner et al. 1993).

Neuronal properties in V2

ORIENTATION. Of the 149 cells from which we collected quantitative data, 41 (28%) were classified as unoriented, 17 (11%) as orientation biased, and 91 (61%) as orientation selective. This is in good agreement with Zeki's (1978) report. Figure 3, A and B, plot the distribution of preferred orientations and orientation half-widths of all V2 cells; unoriented cells are plotted in the bin marked "U". Whereas all orientations are represented in V2, there seem to be more cells whose preferred orientation is closer to vertical

(0 or 180°) than to horizontal or oblique angles, although a χ^2 test showed this orientation anisotropy not to be significant (χ^2 , 9.45; df, 5). Mansfield (1974) and DeValois et al. (1982b) have shown more cells in V1 tuned to vertical/horizontal in the fovea but not the periphery. Whereas this anisotropy was slightly more pronounced in our foveal sample, in no group of cells did it reach statistical significance. Orientation half-widths in V2 ranged from 13° to >90°, with the median being 29°.

We also computed a direction index by taking the ratio of responses (minus baselines) in the nonpreferred to preferred directions and subtracting that ratio from 1. Thus a completely nondirectional cell will have a directional index of 0, and a completely directional unit will have an index of 1. Indices >1 indicate that the cell was inhibited by gratings drifting in the nonpreferred direction. Figure 3C shows the distribution of directional indices for all V2 neurons. Unoriented cells have been included; for these cells we compared the largest responses ~180° apart. Directional cells have been defined here as those cells that responded ≥3 times

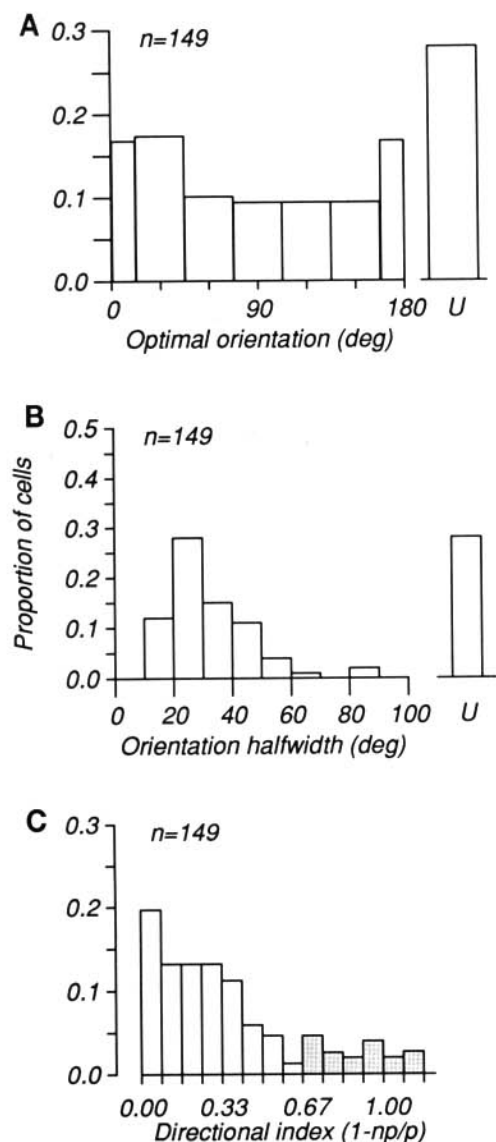


FIG. 3. Orientation and direction selectivity of the entire V2 sample. *A*: distribution of optimal orientations. U, unoriented cells. *B*: distribution of orientation half-widths for the same sample (median = 28.8 deg). *C*: distribution of directional indices for all cells. Direction-selective cells (□) with indices exceeding the criterion (responses that were 3 times greater in the preferred direction than in the nonpreferred). Indices >1 indicate response inhibition by motion in the nonpreferred direction.

better to drift in the preferred direction than to the nonpreferred direction. This corresponds to a directional index of 0.67. Directional cells, shaded in the figure, represent a rather small percentage of the total cell population in V2, ~15% (23/149).

SPATIAL FREQUENCY. Figure 4 plots the distribution of preferred spatial frequencies, cutoff spatial frequencies, and spatial frequency bandwidths. Spatial frequency optima ranged from <0.1 cycles/° up to 7 cycles/°, with a geometric mean of 1.4 cycles/°. Those cells with the lowest spatial frequency optima were low-pass, and some responded well to modulation of a uniform field. These low-pass cells made up ~20% of the V2 population. The spatial resolution of V2 neurons ranged from 1 to 35.5 cycles/° with a geomet-

ric mean of 5.0 cycles/°, and the spatial frequency bandwidths of most cells were between 1 and 5 octaves, with a mean of 2.4 octaves.

TEMPORAL FREQUENCY. Figure 5 illustrates the temporal frequency-tuning characteristics of V2 neurons. V2 temporal frequency optima ranged from <0.5 Hz up to 18 Hz with a geometric mean of 3.2 Hz. Although V2 cells preferred slow drift rates, many were still responsive to high temporal frequencies. The mean temporal resolution was 20.9 Hz; some V2 cells were still responsive to stimuli drifting faster than 32 Hz. V2 neurons were broadly tuned for temporal frequency; bandwidths ranged up to 5 octaves and the mean temporal frequency bandwidth was 3.2 octaves. More than 40% of the V2 population was low-pass for temporal frequency.

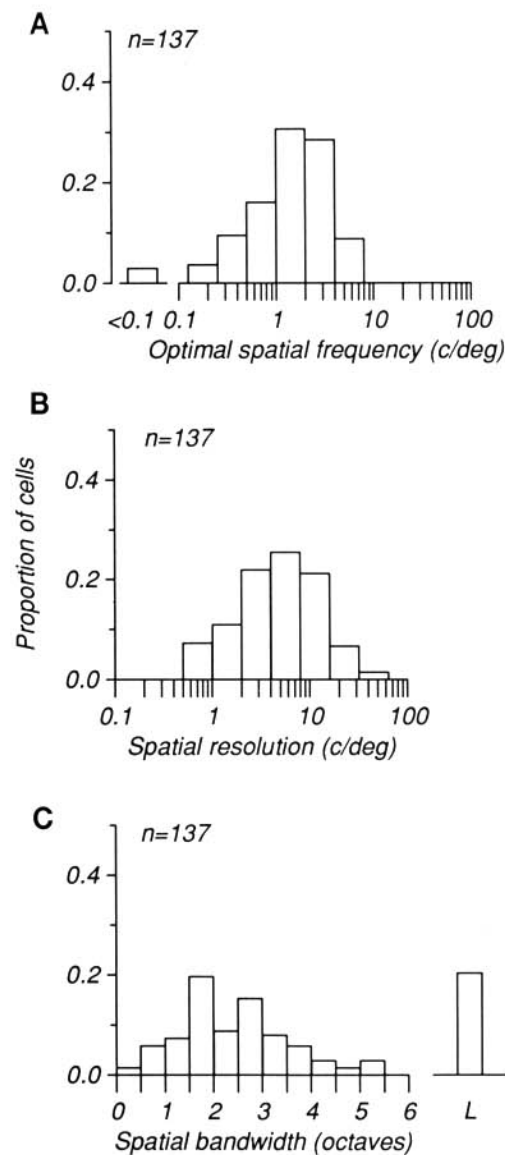


FIG. 4. Spatial properties of the entire V2 sample. *A*: distribution of optimal spatial frequencies (geometric mean = 1.4 cycles/°). *B*: distribution of spatial resolution (geometric mean = 5.0 cycles/°). *C*: distribution of spatial bandwidths (mean = 2.4 octaves). L, low-pass cells for which no bandwidth could be calculated.

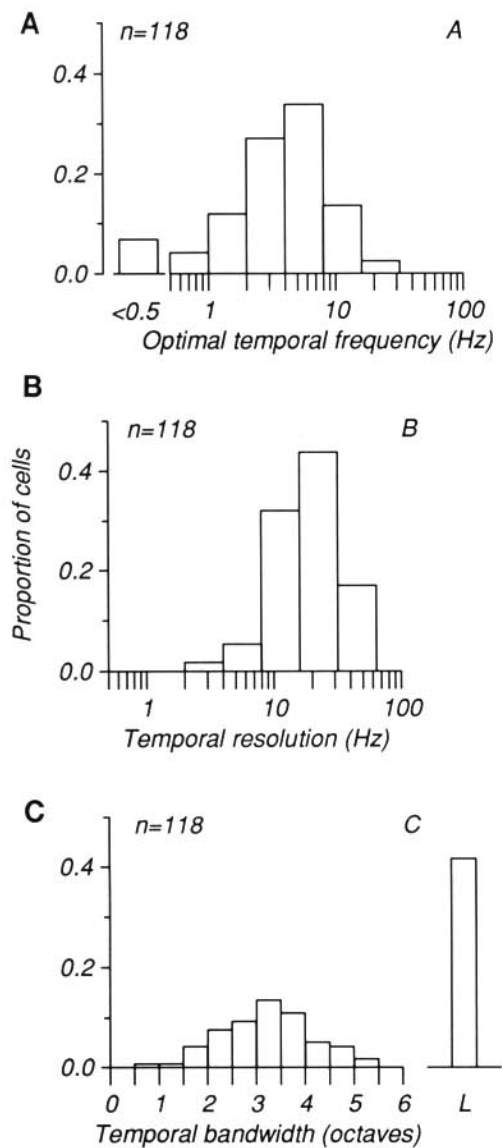


FIG. 5. Temporal properties of the entire V2 sample. *A*: distribution of optimal temporal frequencies (geometric mean = 3.2 Hz). *B*: distribution of temporal resolution (geometric mean = 20.9 Hz). *C*: distribution of temporal bandwidths (mean = 3.2 octaves). L, low-pass cells for which no bandwidth could be calculated.

CORRELATION BETWEEN SPATIAL AND TEMPORAL CHARACTERISTICS. We also examined the V2 population to determine if there was any systematic relationship between a neuron's spatial and temporal tuning. It has been suggested that the two pathways through V2 ultimately derive their predominant excitatory drive from either the P or M divisions of the LGN. In the LGN, although there is much overlap of response properties, those neurons having the best spatial resolution tend to have lower temporal resolution (P), whereas those neurons having the best temporal resolution have somewhat lower spatial resolution (M) (Derrington and Lennie 1984; Kaplan and Shapley 1982; Sherman et al. 1984). This is consistent with the behavioral results of Merigan and Maunsell (1990) and Merigan et al. (1991), showing the importance of the P system for detection of high spatial/low temporal frequency stimuli and the M system

for low spatial/high temporal frequency stimuli. We observed no significant correlation between a neuron's spatial and temporal resolution ($r = 0.16$), nor between cells' *optimal* spatial and temporal frequencies ($r = 0.04$). This suggests convergence of P and M signals in V2. However, we should note that there is some disagreement concerning spatial resolution differences between P and M cells. Hicks et al. (1983), among others, have argued that although M cells have larger field sizes and prefer lower spatial frequencies, their higher contrast sensitivity maintains their responsiveness to high spatial frequencies, so there is in fact no spatial-resolution difference between M and P cells. The lack of correlation seen here may simply reflect this fact.

SPATIOTEMPORAL INTERACTIONS AND SPEED SENSITIVITY. In addition to determining a spatial frequency-response function at the optimal temporal frequency, for some neurons we also made measurements of spatial tuning across a range of temporal frequencies, to determine if the spatial and temporal frequency tuning of these cells were independent (as seems to be the case in V1), or if there were interactions causing spatial frequency tuning to depend on the temporal frequency of the stimulus. Figure 6*A* shows the results of an experiment in which both spatial and temporal frequency were varied. Each curve represents a spatial frequency-response function measured at a different temporal frequency; Fig. 6*B* shows a similar family of curves for a different cell. These plots show that the optimal spatial frequency did not vary in any systematic way across temporal frequency. This suggests that V2 cells' spatial and temporal frequency tuning may be independent, as in V1. We devised an analysis to examine this more rigorously.

The data of Fig. 6*A* are replotted in Fig. 6, *C* and *D*. Figure 6*C* is a three-dimensional perspective view of the entire spatiotemporal response surface. In this plot, the two axes are spatial and temporal frequency, and the height of the surface above the base plane represents response magnitude. The plot in Fig. 6*D* is a contour map of the same surface. Each line in the contour map represents a locus of constant-response magnitude. A cell with spatial and temporal tuning that are independent would produce a response surface and contour map oriented along cardinal directions, vertically or horizontally. This is merely another way of showing that the optimal spatial frequency does not depend on temporal frequency. A cell in which optimal spatial frequency depends on temporal frequency would have a surface whose axis of elongation points obliquely in this spatial frequency-temporal frequency plot.

There are many ways in which spatiotemporal interactions could produce a tilt in the spatiotemporal frequency-response surface. However, one possibility is of special interest and leads to a straightforward prediction. That prediction is of selectivity for the *speed* of a stimulus. A cell tuned to the speed of a stimulus, rather than its spatiotemporal frequency, will produce a response surface tilted with a slope of 1 in this log-log spatiotemporal surface. This follows from the relation that speed is equal to temporal frequency divided by spatial frequency. A line of constant speed is a line of slope 1; lines located in the upper left corner of the log SF-log TF surface denote loci of constant high speed, and lines in the lower right corner represent loci

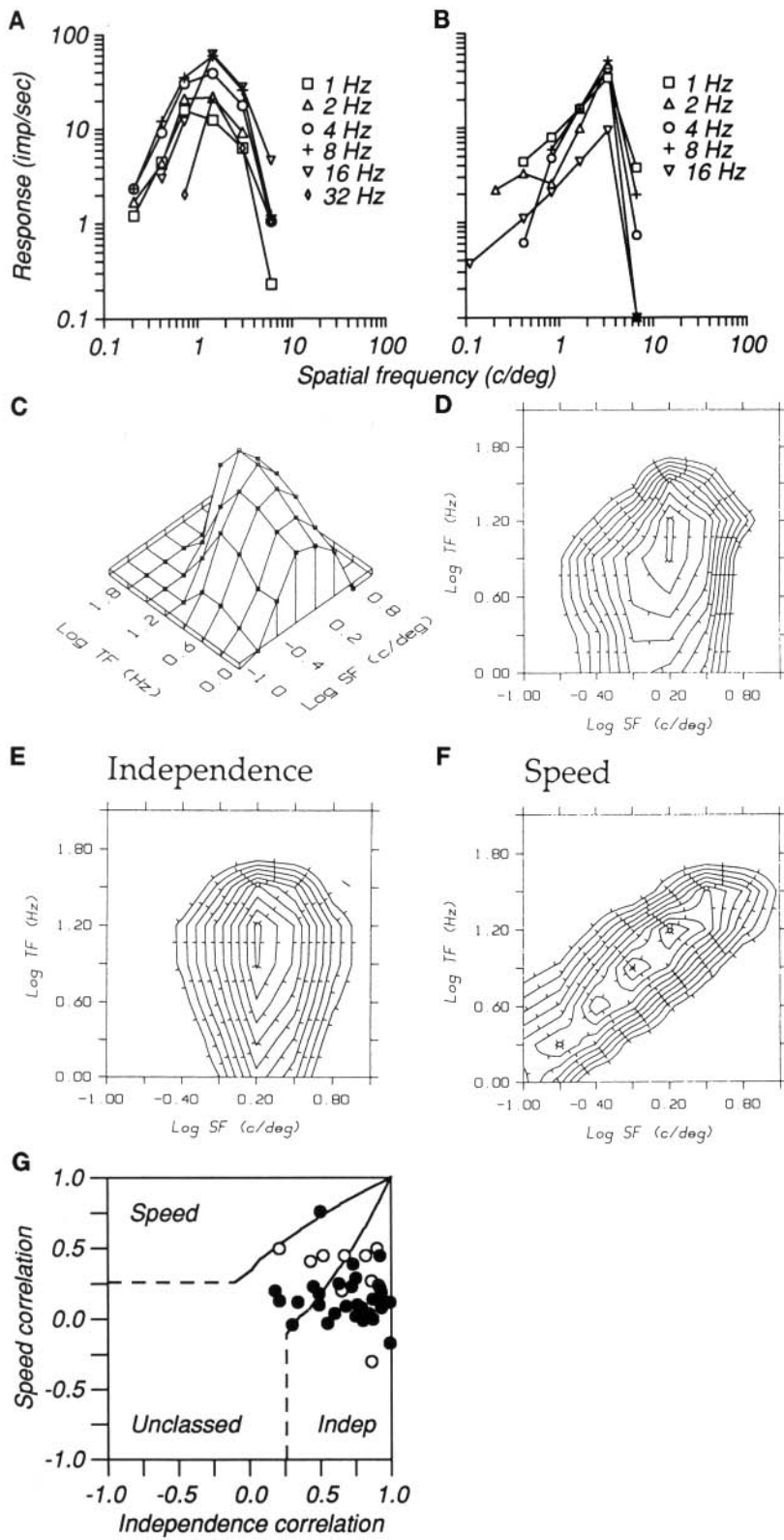


FIG. 6. Spatiotemporal interactions. *A* and *B*: spatial frequency responses of 2 cells measured over a range of temporal frequencies. *C*: three-dimensional response surface representation of the data from *A*. The *x* and *y* axes represent spatial and temporal frequency, and the height above the base plane represents response magnitude. *D*: contour plot of the same data. Each line indicates a line of constant response magnitude; lines are spaced at $\sim 9\%$ of the peak response amplitude. Tick marks point down the surface toward regions of lower response. *E*: contour plot of the predicted spatiotemporal independence surface (see text) generated from the data in *A*. *F*: speed prediction surface (see text) generated from the same set of data. *G*: scatter plot of the partial correlations of 43 V2 cells with the independence and speed predictions. Region below which correlation values are not significantly different from 0 (---) and region within which correlations of the two predictions are not significantly different from one another (-; $P < 0.1$) are marked. Cells having a high correlation with one prediction and a low correlation with the other fall into the regions marked "Speed" or "Independence". Cells whose responses are noisy or inconsistent fall into the lower region marked "Unclassed". Directional cells, \circ ; nondirectional cells, \bullet .

of constant low speed. V2 cells are tuned to the speed of stimuli (Burkhalter and Van Essen 1986; Orban et al. 1986) as are cells in area MT (Maunsell and Van Essen 1983a), and there is evidence that some cells in MT covary their spatial and temporal frequency tuning (Movshon et al. 1988) in the manner described.

We sought to analyze such data that would take into account the entire response surface, not merely the shift of the peak response points. We did this by generating two prediction surfaces and then computing the partial correlation of the actual response surface with each of the two alternative predictions. This analysis is analogous to that used by Mov-

shon et al. (1985) to analyze MT cell responses to compound-motion stimuli. From the response matrix, we extracted the spatial frequency-response curve and the temporal frequency-response curve passing through the overall peak response point. These correspond to the spatial frequency response measured at the optimum temporal frequency, and the temporal frequency response measured at the optimum spatial frequency. The first prediction, spatio-temporal independence, was generated by taking the spatial frequency-tuning function and simply replicating it at different temporal frequencies, scaled by the temporal frequency-response function. This independence-prediction surface is shown in Fig. 6E. The other prediction, speed tuning, was generated by taking the spatial frequency-response function and replicating a scaled and *shifted* version of it at different temporal frequencies. The speed prediction surface is shown in Fig. 6F.

We next calculated how well the actual response surface was correlated with each of the two predictions. Because the two predictions are not completely uncorrelated themselves, we used a partial correlation of the form

$$R_i = \frac{r_i - r_s \cdot r_{is}}{\sqrt{(1 - r_i^2)(1 - r_s^2)}}$$

where R_i is the partial correlation of the data with the independence prediction, r_s is the correlation of the data with the speed prediction, r_i is the correlation of the data with the independence prediction, and r_{is} is the correlation of the two predictions with each other. The analogous partial correlation with the speed prediction was obtained by interchanging r_i and r_s . The V2 cell shown in Fig. 6 had an independence correlation of 0.92 and a speed correlation of 0.22.

We summarize these data in Fig. 6G. The x -axis indicates independence correlation values and the y -axis indicates speed correlation values. The dashed lines indicate correlation values of 0.258. Correlation values that fell within the region bounded by these dashed lines were not significantly different from zero ($P < 0.1$). Points that fell inside this region, marked "unclassified", represent responses that were noisy or inconsistent and thus lead to low correlation values for both predictions. The region bounded by the solid curve in the upper right corner of this plot represents cells whose responses correlated well with both predictions. In this region, correlations for the two predictions were not significantly different from one another ($P < 0.1$). These data are uninterpretable in the present context and may reflect the degree to which the two predictions are themselves correlated. Neurons whose responses were well correlated with one prediction, but poorly or negatively with the other fall into the two regions marked "independence" or "speed".

We calculated these partial correlation values for 43 V2 cells. Figure 6G is a scatter plot of independence correlation versus speed correlation. The scatter plot shows that almost all V2 cells' responses are better correlated with the independence prediction than with the speed prediction. We expected that if any cells were to show a significant correlation with the speed prediction, they would be the directional cells, because the only neurons that seem to behave in this manner are directional cells found in MT (Movshon

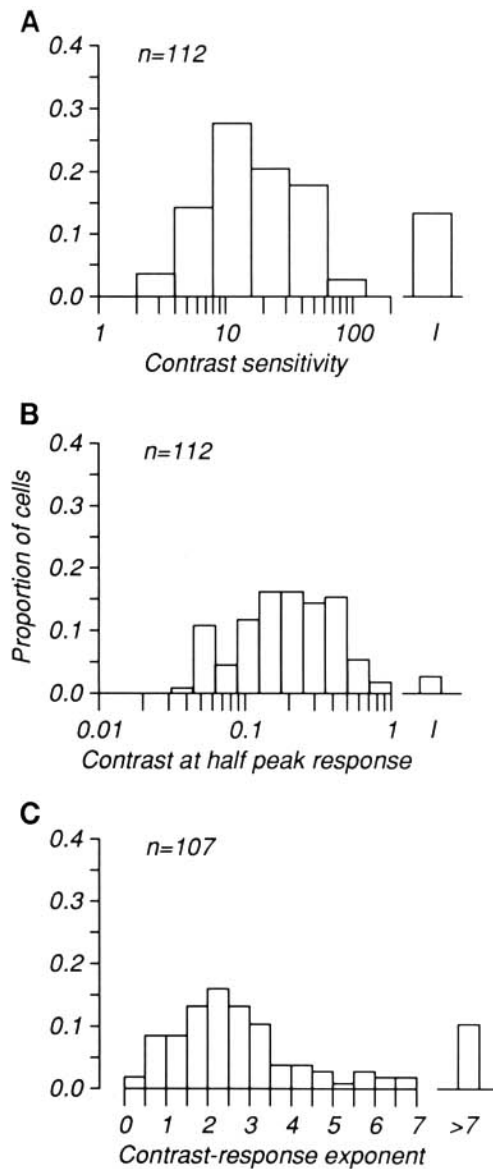


FIG. 7. Contrast response properties of the entire V2 sample. A: distribution of contrast sensitivity—defined as the reciprocal of threshold contrast (defined in the text; geometric mean = 0.164). Insensitive or unresponsive cells are plotted in I. B: distribution of semisaturation contrasts for the same sample (geometric mean = 0.186). Because the semisaturation constant can lie outside the range of the data, these contrasts do not represent those required for half the maximum response actually observed. C: distribution of exponents, i.e., slope of contrast response function (geometric mean = 2.66; data from unresponsive units not included). B and C are derived from hyperbolic fits to contrast response data.

et al. 1988). In Fig. 6G, the open symbols represent directional cells and closed symbols represent nondirectional cells. Although directional cells were in fact among those cells with the highest speed correlations, there was extensive overlap of the nondirectional and directional cell populations, and no cell could be classified as a speed cell by this method. Those directional cells that did have the highest speed correlations were also well correlated with the independence prediction. These cells are plotted in the upper right corner of the plot, and no firm conclusions can be drawn about them.

CONTRAST SENSITIVITY. Figure 7*A* illustrates the distribution of contrast sensitivities for the entire sample. Units that failed to reach the criterion probability level are counted in the bin marked “I” (for insensitive). Contrast sensitivities ranged from ~ 3 up to 100, with a geometric mean of 16.4. These sensitivity values correspond to threshold contrasts from 0.01 for the most sensitive cell to 0.33 for the least sensitive, with a mean threshold contrast of 0.06. Figure 7, *B* and *C*, illustrates the distributions of semisaturation contrasts and exponents (that govern the steepness of the contrast response function). Most V2 cells’ semisaturation contrasts were <0.40 ; the geometric mean for all cells was 0.19. The observed values of exponents ranged from <1 to >7 with a geometric mean of 2.66.

RELATION BETWEEN CONTRAST SENSITIVITY AND DIRECTION SELECTIVITY. If there is a segregation of P and M signals through visual cortex, then directional cells might have higher contrast sensitivity than nondirectional cells, as directional cells are situated in regions in both V1 (layer 4b) and V2 (thick stripes) that are part of an M pathway through visual cortex. Directional cells tended to have the highest contrast sensitivities, but some nondirectional cells were equally sensitive. Although there was a small positive correlation between contrast sensitivity and directional index, it was not statistically significant. What distinguished directional cells from nondirectional cells was the absence of direction-selective cells with low-contrast sensitivities. This is similar to what was found in V1 by Hawken et al. (1988), and also may indicate convergence of P and M signals in cortex (although higher sensitivities could plausibly result from convergence of P signals alone).

CHROMATIC PROPERTIES. We made quantitative measurements of the chromatic properties of 50 V2 neurons. Our aim was to establish a reliable measure of cells’ relative responsiveness to chromatic versus achromatic stimuli, which might serve to distinguish what others have described as “color” cells. We measured responses to modulations in each of the three principal planes of the color space and used gratings of the optimal spatial frequency as well as uniform fields. Some cells responded to uniform fields whose luminance or chromaticity were modulated in time. As in the LGN and in V1 (Derrington et al. 1984; Lennie et al. 1990), the characteristic elevation (θ_m) of V2 cells dropped when uniform field stimuli were used. The following description of cells’ chromatic properties therefore is based on measurements using gratings of the optimal spatial frequency. Almost all V2 neurons were more responsive to luminance modulation than to any purely chromatic modulation. Figure 8*A* is a summary figure of the chromatic properties of our sample; we include only those 37 cells whose responses could be fit by modified sinusoids. An additional five cells’ responses were poorly fit, and the remaining eight cells responded too inconsistently to include in this analysis. The θ_m for each cell is plotted against its ϕ_m . Because of how this space is defined, ϕ values become undefined as θ approaches 90°. This figure shows that most V2 cells responded best to stimulus modulations elevated well out of the isoluminant plane, i.e., they were more responsive to variations in luminance than in chromaticity. Furthermore these neurons’ ϕ_m values were spread uni-

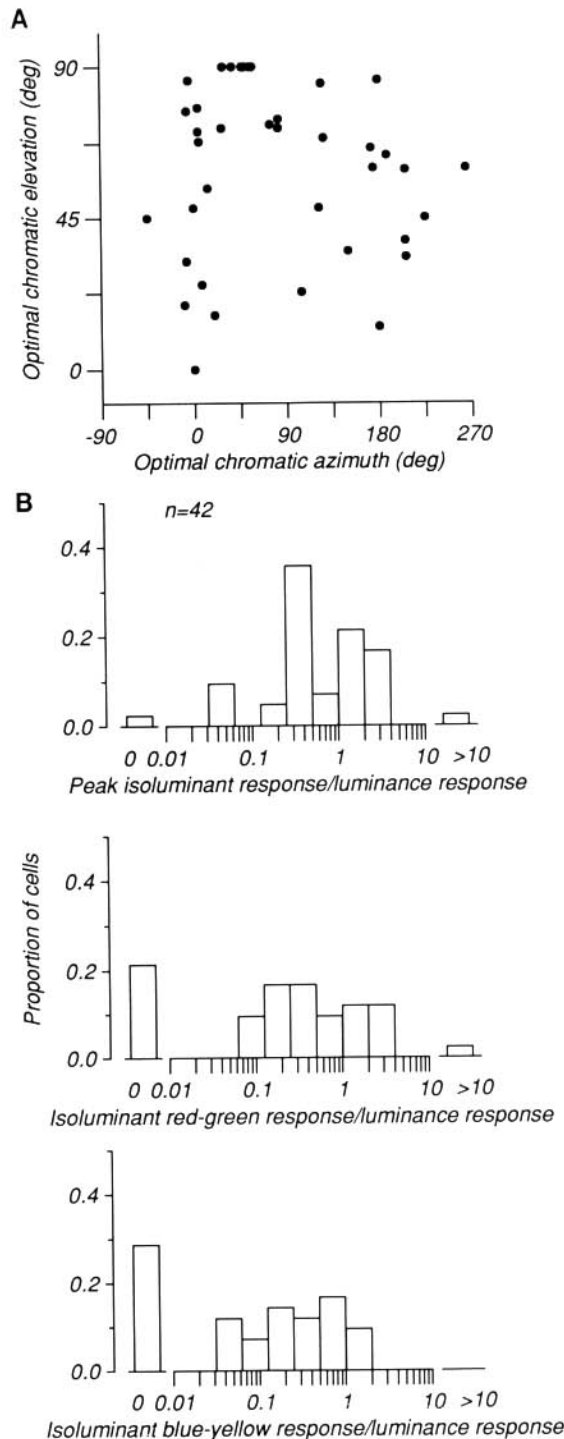


FIG. 8. Chromatic properties of the entire sample. *A*: summary diagram showing θ_m and ϕ_m for the 37 cells satisfactorily described by (modified) sinusoidal fits. Elevation of 0° represents isoluminant chromatic modulations, and elevation of 90° represents pure luminance modulation. Azimuths of 0° and 180° represent red-green modulations, whereas azimuths of 90° and 270° represent blue-yellow modulations. *B*: distribution of response ratios. Peak response in the isoluminant plane divided by luminance response, *top*; isoluminant response along the red-green axis divided by luminance response, *middle*; isoluminant response along the blue-yellow axis divided by luminance response, *bottom*. Most cells have ratios <1 , indicating that they are more responsive to luminance modulation than to isoluminant color modulations. A ratio of 0 indicates that the cell gave no response to isoluminant color modulations.

formly from 0 to 180°. Those cells with low elevations were more responsive to variations in chromaticity, and they seemed to cluster around an ϕ_m of 0°, i.e., they preferred modulations between red and green, although we did find a few cells that responded to blue-yellow modulations.

Because some response data were not well described by sinusoids, we also used a description of cells' chromatic properties that is independent of any fits to the data. For each cell, we determined the ratio between the peak response in the isoluminant plane and the response to purely luminance modulations. We also determined this ratio along the cardinal RG and BY axes in the isoluminant plane. Figure 8B illustrates the distributions of these ratios. In agreement with our other analysis, most cells had ratios <1, i.e., they were more responsive to luminance variations. We note that this result, and the relative responsiveness of cells to different isoluminant color stimuli, also might reflect the relative scaling of axes in color space that we chose; however, we encountered *no* cell that did not respond to luminance stimuli. Of those cells that responded to isoluminant color variations at least as well as to luminance, fewer responded to blue-yellow modulations (9%) than to red-green (26%), and a substantial number of cells were most responsive to modulations along neither of these axes.

In most cases, our qualitative classification of cells as color selective agreed with subsequent quantitative measurements; of the 13 cells mapped as color cells from which we also made chromatic measurements, 10 (77%) responded well to isoluminant color variations. We also found, in agreement with previous work in V2 (Baizer et al. 1977; Hubel and Livingstone 1987) that color selectivity and poor orientation selectivity were often associated. Of the 17 cells whose best response to isoluminant color variations was equal to or greater than the best luminance response, 8 (47%) were unoriented, whereas of the total V2 population, 28% were unoriented. [Of the 11 cells with optimal elevations within 45° of the isoluminant plane, 6 (55%) were unoriented.] Conversely, of the 16 unoriented cells whose chromatic properties we measured, 8 (50%) responded to isoluminant color modulations as well as or better than pure luminance stimuli.

SIMPLE AND COMPLEX CELLS. In the course of these experiments, we also noted a group of simple cells similar to those found in V1. Most cells in V2 were like V1 complex cells, responding to drifting grating stimuli with an essentially unmodulated elevation of their firing rate. Simple cells in V1 respond to drifting gratings with a modulation of their discharge at the same temporal frequency as the stimulus. Complex cells, however, only exhibit this modulation at the lowest spatial frequencies and rarely show modulation at the cell's optimal spatial frequency (Movshon et al. 1978a,b). In Fig. 9A are plotted the response histograms of two V2 cells during one drift cycle for a range of spatial frequencies straddling each cell's optimal spatial frequency. The complex cell responded to all spatial frequencies with an unmodulated elevation in its firing rate. The simple cell responded to all spatial frequencies with a discharge modulation in synchrony with the stimulus.

The modulation index for these cells is the ratio of the

first harmonic of the cell's response to its average firing rate minus the baseline, measured at the cell's optimal spatial frequency. The complex cell of Fig. 9A had a modulation index of 0.09, and the simple cell an index of 1.30. Figure 9B plots the distribution of this index for all V2 cells for which we made full spatial frequency-tuning measurements. In V1, this measure is bimodally distributed (DeValois et al. 1982a; Skottun et al. 1991), with the separation between the two groups occurring at a value of 1. Those cells with modulation indices >1 are the simple cells, and those <1 are the complex cells. In V2, we found the unimodal distribution seen in Fig. 9B, which falls off monotonically from 0. Simple cells are indicated by the shaded histograms. For these cells, we did not use average firing rate as the response measure. Instead we used the amplitude of response modulation at the fundamental temporal frequency of the stimulus. This group was a sizable portion of the entire V2 sample, ~25% (37/137). We sampled receptive fields as far peripheral as 9° and encountered only 3 simple cells (of a sample of 23) beyond 3°. However, although we did sample all laminae beyond 3°, we cannot be certain that the bias toward complex cells at eccentricities beyond 3° is not because of sampling.

Because the modulation index does not cleanly distinguish simple and complex cells, as it does in V1, we wondered whether these were in fact distinct cell types, and if any properties were correlated with modulation indices >1. The first evidence for this is the distinct localization of these cells within V2. We encountered simple cells mainly in the representation of the central 3 deg—30% (34/114) of the population within 3°, 13% (3/23) beyond. In addition, these cells seemed to have a specific laminar localization within V2. Simple cells, though found in all laminae, were encountered most frequently in the upper and middle layers of cortex. In layers 2–4, simple cells formed roughly one-third of the population, whereas in the infragranular layers, they made up only ~10%. Furthermore it was the cells in the primary V1 input layers, layers 3B and 4, that had the highest modulation indices. Within the central 3°, simple cells also had somewhat smaller receptive field diameters than complex cells, 0.81 versus 1.05 deg.

In addition, the response properties of these two groups of cells differed in a way reminiscent of the differences seen between these two groups in V1. Simple and complex cells' temporal tuning and contrast sensitivity were found to be essentially identical. Their spatial properties, however, differed rather dramatically. As in V1, V2 simple cells were tuned to significantly lower spatial frequencies and had lower spatial resolution than did complex cells. Figure 9C shows the distribution of spatial resolution for V2 simple and complex cells. Simple cells had a geometric mean spatial resolution of 2.3 cycles/°, whereas complex cells' geometric mean spatial resolution was 6.3 cycles/°. Simple cells' geometric mean optimal spatial frequency was 0.6 cycles/° and that of complex cells was 1.8 cycles/°. Both differences between the two groups were highly significant (spatial frequency optima, $U = 664$, $z = 5.63$, $P < 0.001$; spatial resolution, $U = 570$, $z = 5.85$, $P < 0.001$). Foster et al. (1985) also have observed differences in the spatial properties of V2 simple and complex cells, and these differences also are seen in V1 (DeValois et al. 1982a; Foster et al.

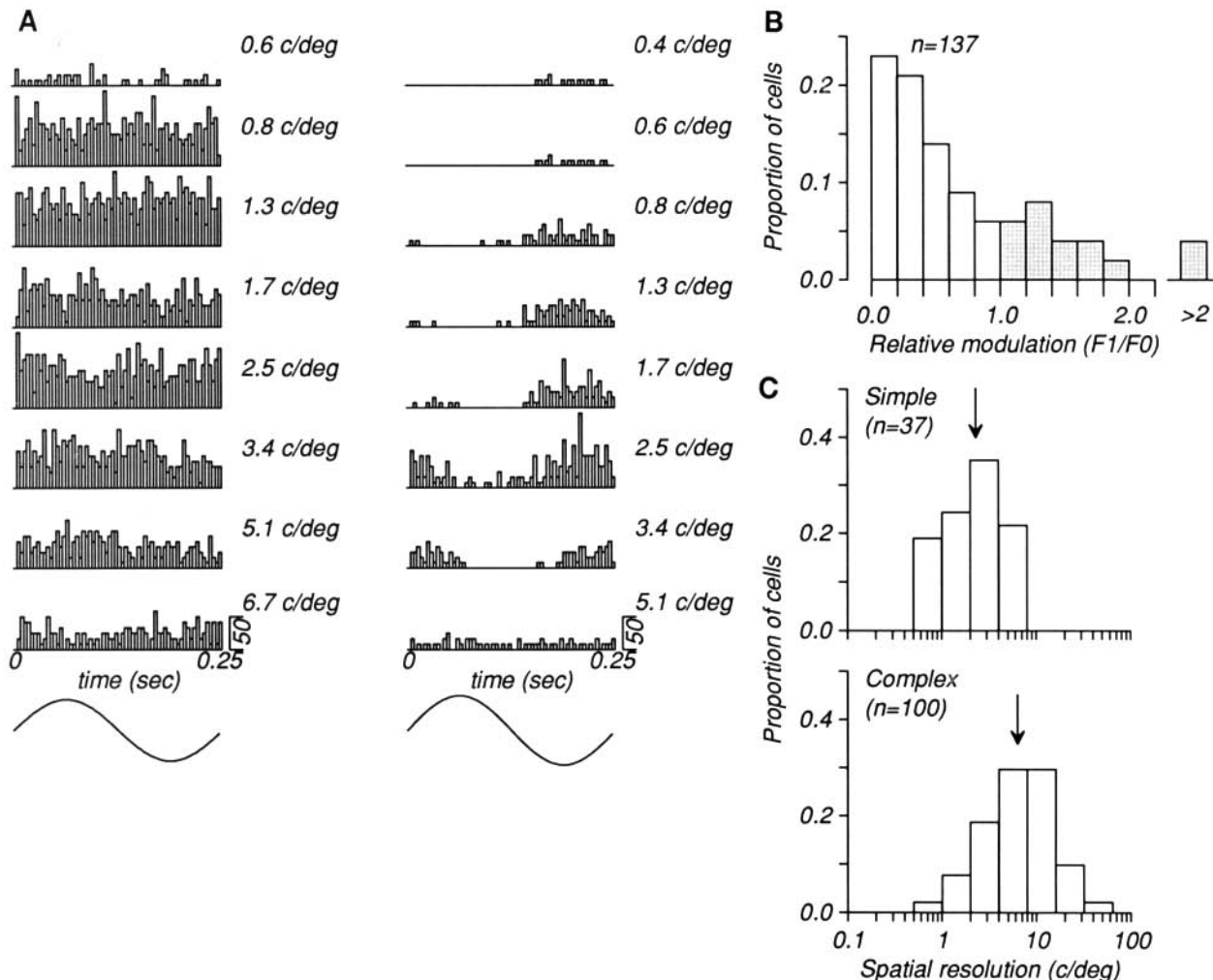


FIG. 9. Simple and complex cells. *A*: peristimulus time histograms of 2 V2 cells during the time 1 cycle of a grating drifted across their receptive fields. Each row represents responses to a different spatial frequency (*right* of each histogram). The responses on the *left* belonged to a complex cell that responded to all spatial frequencies with an unmodulated elevation of its discharge rate. The responses on the *right* belonged to a simple cell that responded with a modulation of its firing in synchrony with the drift of the grating. Calibration bar represents 50 impulses/s. *B*: distribution of relative modulation (defined as the first harmonic of the cell's response divided by the mean firing rate with baseline subtracted, measured at the cell's optimal spatial frequency) for all V2 cells. A criterion value of 1 divides simple and complex cells. Simple cells, □. *C*: spatial resolution of simple and complex cells. Complex cells resolved significantly higher spatial frequencies. Geometric means (↓): simple cells, 2.3 cycles/°; complex cells, 6.3 cycles/°.

1985). These differences in localization and properties suggest that the simple/complex distinction may be valid in the foveal representation in V2.

Anatomic distribution of response properties within V2

In the preceding section, we described the response properties of V2 neurons without regard to their location in V2. We wished to relate these properties to the CO-defined architecture of V2. Previous research has emphasized the inhomogeneous distribution of neurons having such distinctive response properties as end stopping, directional selectivity, color selectivity, and lack of orientation selectivity (DeYoe and Van Essen 1985; Hubel and Livingstone 1987; Shipp and Zeki 1985). We therefore explored the distribution of neurons having these special attributes in different CO compartments. In addition, many orientation-selective neurons in our sample lacked any of these distinctive fea-

tures, and we refer to these as "vanilla" cells. Because vanilla cells were common in all CO compartments, we also have analyzed the response properties of *all* the neurons in each compartment without regard to their particular receptive-field attributes, to establish whether the overall distribution of neuronal properties clearly distinguished different CO compartments.

CLUSTERING OF RECEPTIVE-FIELD PROPERTIES. Figures 10 and 11 illustrate representative electrode penetrations through V2, and demonstrate the clustering of receptive-field properties often seen in penetrations through V2.

Figure 10*A* shows a penetration that entered V2 near the lip of the lunate sulcus in a dark compartment that contained color-selective and unoriented cells, then passed through the white matter, and reentered grey matter in another dark compartment that contained a cluster of two clearly directional cells and two directionally biased units. Note that commingled with the directional cells were an

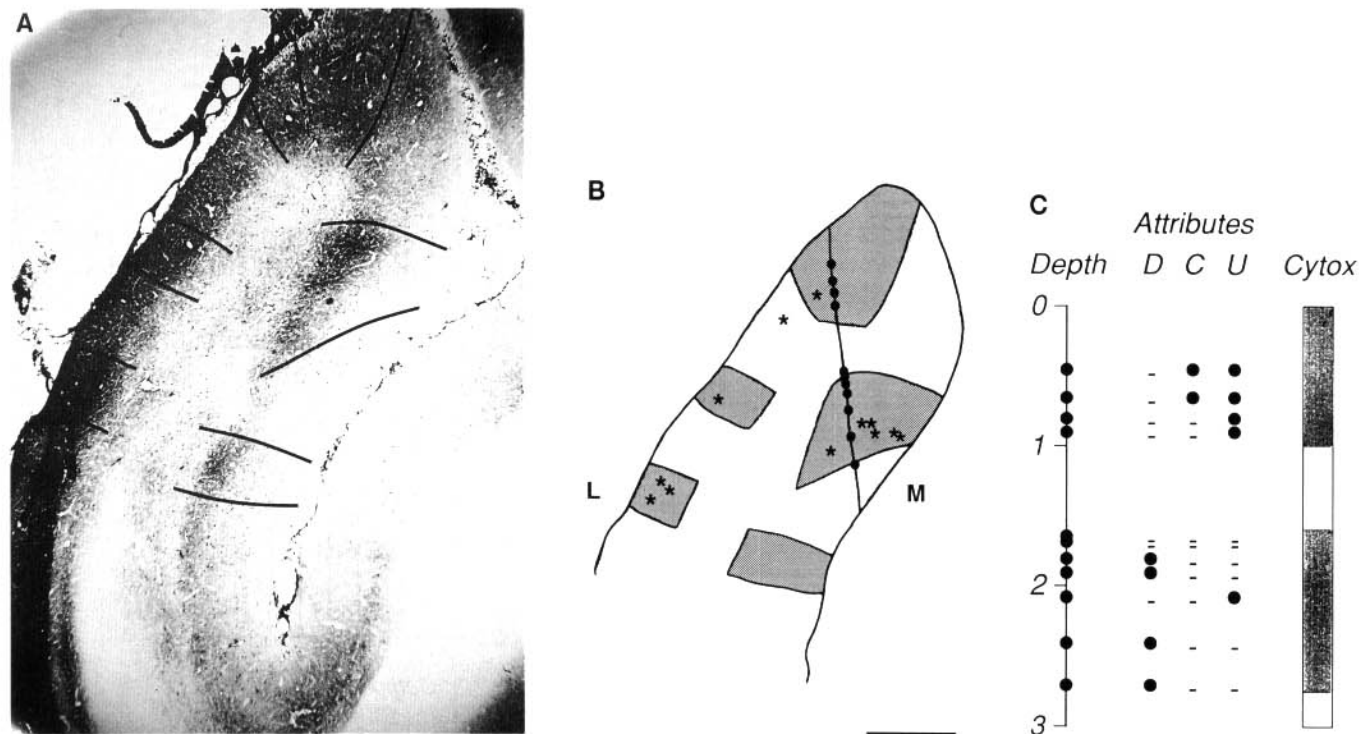


FIG. 10. *A*: photomicrograph of a representative electrode penetration through V2 (tissue stained for CO), with the different CO compartments outlined. The electrode entered V2 at the lip of the lunate sulcus in a dark stripe (thin) that contained all color-selective and unoriented cells, then passed through the white matter, and reentered grey matter in another dark stripe (thick) containing several directional cells. Note the unoriented cell among the directional cells. *B*: schematic drawing of the same electrode penetration. Recording sites, (●); CO-rich compartments, (□); Cat-301(+) cells, ★; L = lateral; M = medial; scale bar = 1 mm. *C*: schematic figure of receptive-field properties encountered. *C*, color selective; DS, direction selective; U, unoriented; depth-column recording sites, ●. In attributes column, cells with that attribute (●) and without (○) are indicated.

unoriented unit and three vanilla cells. Figure 10, *B* and *C*, is a schematic that indicates the progression of receptive-field properties encountered along the penetration, and the location of Cat-301 cells in this tissue section. In the cases shown in Figs. 10 and 11, CO-stained tissue sections were later counterstained for Cat-301. Whereas Cat-301 cells were generally clearly distinguishable from CO cells (for example by the membrane-restricted localization of staining), they did not show up clearly in photographs. We have chosen therefore to indicate their positions in the schematic drawings. In these schematics, we indicate as Cat-301 cells only those clearly distinguishable from the background CO staining; as noted in METHODS, the absolute number of Cat-301 cells also seemed somewhat lower in counterstained material. Although a few lightly labeled Cat-301 cells were found in the first recorded CO-dark stripe, they were clearly more numerous and more intensely labeled in the second stripe, consistent with our identification of this compartment as a thick stripe.

Figure 11*A* illustrates another penetration, which entered V2 in a dark stripe containing a cluster of unoriented and color-selective cells and then passed through a pale region near the V1 border that contained mostly vanilla cells. After passing through the white matter, the electrode reentered V2 in a region in which CO staining was too variable to make unequivocal stripe identifications; at the bottom of the penetration, another dark region consisting almost entirely of directional cells was encountered. In this case as

well, Cat-301 labeling was clearly more prominent in the dark zone at the base of the penetration, again consistent with its identification as a thick stripe.

One feature of V2 that became apparent is that although there is a tendency for cells with certain properties to cluster together in certain CO compartments, this tendency was not absolute. A cell with any particular qualitative selectivity could be found in *any* compartment in V2. For example, we often found unoriented cells scattered among a run of directional cells, or a directional cell amidst a group of color-selective cells. This feature can also be seen in the data of DeYoe and Van Essen (1985). It also became clear that a common type in *all* compartments was the vanilla cell, i.e., a nonend-stopped-oriented cell without any selectivity for the color or direction of motion of a stimulus.

QUANTITATIVE DIFFERENCES IN RECEPTIVE-FIELD PROPERTIES. Although neurons with qualitatively different selectivities did seem to cluster together into different cytochrome oxidase-defined regions, we also were interested to know if the cells in those regions having particular selectivities differed quantitatively in their spatial, temporal, contrast, or chromatic-response properties. The following figures describe the properties of 113 neurons that we could localize to particular CO compartments. This analysis is based on 15 penetrations in 10 hemispheres, with a mean track distance of 3.4 mm (sufficient to span a complete CO stripe cycle of 3–4 mm). Although we do use statistical tests

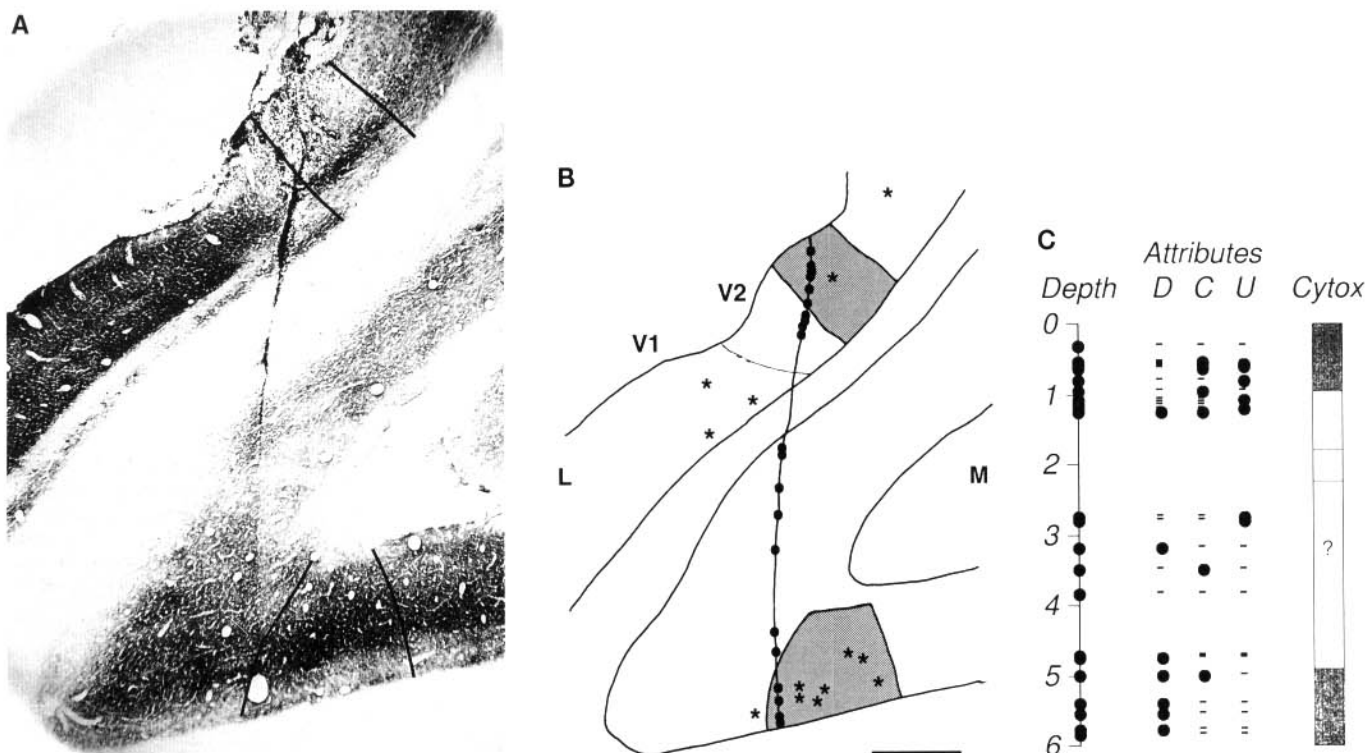


FIG. 11. Photomicrograph *A* and schematics *B* and *C* of another representative electrode penetration. Schematics as in Fig. 10; scale bar = 1 mm. This penetration entered V2 in a dark stripe (thin) that contained color-selective and unoriented cells, then passed through a pale region at the border with V1 containing a cluster of vanilla cells. The electrode reentered V2 in another pale region, then went through cortex in which the staining was too variable to make any identification of stripe regions, and ended in a dark stripe (thick) at the base of the lunate sulcus that contained almost exclusively directional cells (next to the large lesion in layer 5). See text for further description.

where appropriate to assess the reliability of quantitative response differences between CO compartments, we do not use such tests to assess differences in the relative proportions of qualitatively different cell types. This is because the small numbers of cells involved reduce the power of such distribution tests or simply render them inappropriate. Given such limitations (the need for either more data or more sensitive statistical tests), we are therefore reluctant to attribute significance to any such differences.

ORIENTATION SELECTIVITY. The most striking difference in the orientation selectivity of the three compartments in V2 was the incidence of clusters of unoriented cells. As noted above, in only one set of stripes (thin), could we find clustered groups of unoriented cells. However, scattered unoriented cells could be found in *any* compartment. The proportion of unoriented cells in each compartment that could be unambiguously identified as thick, thin, or pale were: thick, 12% (3/24); thin, 50% (13/26); pale, 24% (8/33). We also examined the group of oriented cells in each compartment to determine if there were any differences in their orientation selectivity. The median orientation half-widths in each compartment (not including nonoriented cells) were 40.3° in thick stripes ($n = 21$), 28.8° in thin stripes ($n = 13$), and 25.8° in pale stripes ($n = 25$). Although thick stripe cells were somewhat more broadly tuned than other cells, none of these differences was significant.

SPATIAL PROPERTIES. Figure 12*A* shows the distributions of spatial-frequency optima of cells in the compartments of

V2. The mean optimal spatial frequency for thick stripes was 1.4 cycles/°, for thin stripes was 1.0 cycles/°, and for pale stripes was 1.4 cycles/°. None of these differences was statistically significant. A noteworthy feature of this figure is the relatively high proportion of low-pass cells found in the thin stripes. As noted earlier, these spatially low-pass cells were almost all unoriented, and this figure shows that they were most common in the thin stripes. Figure 12*B* shows the distribution of spatial resolution properties of each stripe. The mean spatial resolution of neurons in thick stripes was 5.8 cycles/°, in thin stripes 4.1 cycles/°, and in pale stripes 5.9 cycles/°. None of these small differences was statistically significant. Apart from the low-pass cells, the cells in all three compartments were tuned to the same range of spatial frequencies. There were no differences in the spatial-frequency bandwidths of cells in the stripes. Mean spatial-frequency bandwidth in thick and pale stripes was 2.7 octaves and in thin stripes 2.6 octaves. Because of the high incidence of low-pass cells in thin stripes, however, it is likely that the average neuronal response to very low spatial frequencies would be highest in this compartment.

TEMPORAL PROPERTIES. Figure 13 shows the distributions of optimal temporal frequency and temporal resolution for the three compartments. Mean optimal temporal frequency was 4.1 Hz in thick stripes, 2.8 Hz in thin stripes, and 3.2 Hz in pale stripes. None of the differences was significant. Thin stripes again contained the highest proportion of low-pass neurons, in this case for temporal frequency. Temporally low-pass units were different from spatially

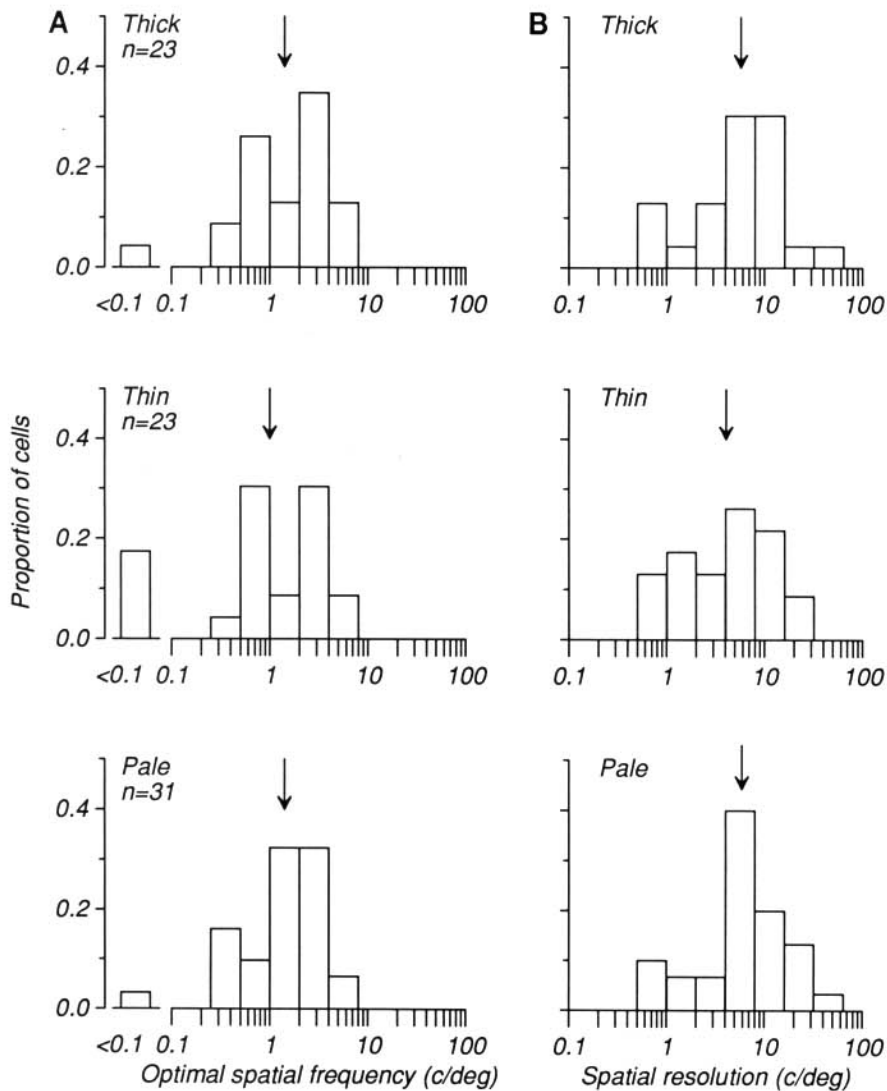


FIG. 12. Distribution of spatial frequency optima and resolution of cells localized to different CO compartments in V2. Geometric means of each distribution are indicated [\downarrow ; SF optima: thick (1.4), thin (1.0), and pale (1.4); SF resolution: thick (5.8), thin (4.1), pale (5.9); all values expressed as cycles/ $^{\circ}$].

low-pass ones in that there was no particular tendency for them to be unoriented. These neurons were as responsive to higher drift rates as neurons in thick or pale stripes, but had no low-frequency rolloff. Figure 13*B* illustrates that cells in the three compartments had the same mean temporal resolution: 18.2 Hz in thick stripes, 17.8 Hz in thin stripes, and 16.6 Hz in pale stripes. None of these differences in temporal resolution was significant. As was the case with the spatial tuning, there were no differences in their selectivity for temporal frequency. Temporal-frequency bandwidths were essentially identical: in thick stripes 3.3 octaves, in thin stripes 3.4 octaves, and in pale stripes 3.0 octaves. None of these differences was significant.

CONTRAST SENSITIVITY. Figure 14 shows the distribution of contrast sensitivities in each compartment. The mean sensitivity in thick stripes was 20.9, in thin stripes 10.9, and in pale stripes 20.0. Cells in the thin stripes were significantly less sensitive than those in thick and pale stripes (thick vs. thin: $U = 90.5$, $z = 2.21$, $P < 0.03$; pale vs. thin: $U = 105$, $z = 2.4$, $P < 0.02$) but thick and pale stripes were not significantly different from one another. We also subdivided the thick-stripe cells into directional and nondirectional groups to examine any possible difference between those groups.

We found that directional cells in the thick stripes were more sensitive than were nondirectional cells (28.8 vs. 14.5). This difference approached but did not reach statistical significance ($U = 27$, $z = 1.74$, $P < 0.08$). In fact, thick-stripe directional cells had the highest mean sensitivity of any group. This sensitivity value corresponds to a threshold contrast value of 0.035; the least sensitive group of cells, those in the thin stripes, had a mean sensitivity corresponding to a threshold contrast of 0.092. This is all in agreement with the data described earlier; directional cells are among those with the highest sensitivities, but nondirectional cells can be equally sensitive. What is surprising is that nondirectional cells in thick stripes were relatively insensitive; in fact, they are less sensitive than pale-stripe cells and not much more sensitive than thin-stripe cells. We also examined the contrast sensitivity of directional cells in pale stripes (none could be unambiguously localized to a thin stripe). Although we measured sensitivity of only four directional cells in pale stripes, two of them had the highest contrast sensitivities of any pale-stripe cell. It thus seems that directional cells may be more sensitive than other cells, regardless of their location.

The distributions of semisaturation constants and expo-

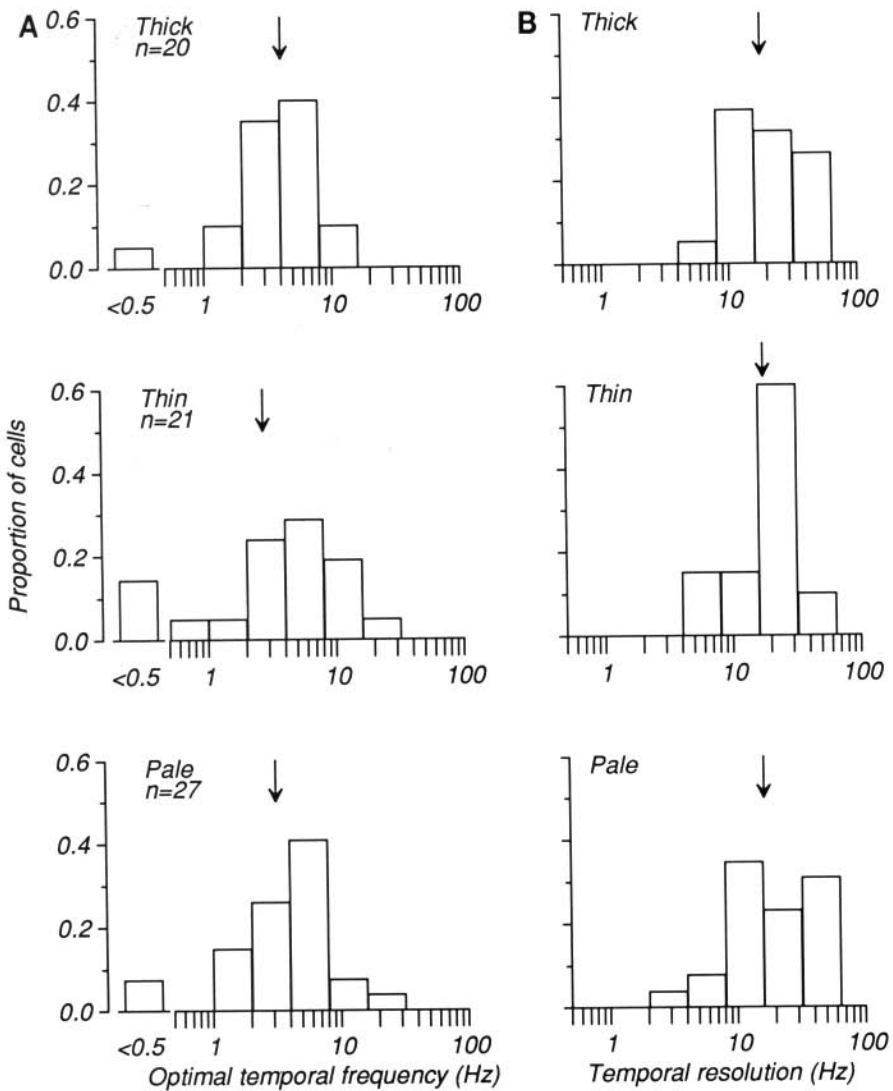


FIG. 13. Distribution of temporal frequency optima and resolution of cells in different CO compartments in V2. Geometric means are indicated [↓; TF optima: thick (4.1), thin (2.8), pale (3.2); TF resolution: thick (18.2), thin (17.8), pale (16.6); all values expressed as Hz].

nents from the contrast response fits confirm and extend these results. The geometric mean values of semisaturations in thick, thin, and pale stripes were 0.16, 0.22, and 0.14, respectively. As above, thick- and pale-stripe cells were most sensitive, having the lowest semisaturations, and thin-stripe cells were less sensitive, indicated by their higher average semisaturations. However, none of these differences was significant. Nor were there significant differences among the exponents governing the steepness of the contrast-response functions. Mean values were 2.66 in thick stripes, 2.45 in thin stripes, and 2.74 in pale stripes.

CHROMATIC PROPERTIES. Of the 42 cells from which we obtained quantitative chromatic data, we were able to localize 20 to particular compartments: 15 in thin stripes, and 5 in pale stripes. Roughly half (8/15) of the thin-stripe cells were more responsive to isoluminant chromatic modulations than to luminance modulations, whereas all pale-stripe cells were more responsive to luminance modulations. This difference also is reflected by the peak isoluminance/luminance response ratio (described above); the median value was 1.2 in thin stripes and 0.4 in pale stripes.

RELATIVE INCIDENCE OF SELECTIVITIES ACROSS V2. The preceding figures have illustrated the response properties of

neurons in different compartments of V2; with few exceptions quantitative differences are rather subtle. Figure 15 plots the relative proportions of cells in each of the three CO compartments having particular qualitative attributes. The darkened portion of each bin indicates the proportion of cells in that compartment having that particular attribute: color selectivity, direction selectivity (DS), end stopping, or orientation selectivity. Because some cells had more than one of these attributes, the total can exceed 100%. Although it is true that color-selective and unoriented cells were found predominantly in the thin and pale stripes, and DS cells in the thick stripes, it should be understood clearly that neurons having *any* qualitative selectivity can be found in *any* compartment. For example, we found several cells displaying a clear color preference that were DS and/or located in thick stripes. Furthermore the clustering we observed did not depend on the precise criteria used to define cell types. For example, we used a strict criterion to define direction selectivity (preferred response ≥ 3 times greater than nonpreferred response); with a looser criterion (1.5:1 or 2:1), more cells were defined as DS in all compartments, but they were still most common in thick stripes.

Figure 16 also plots the relative incidence of cell proper-

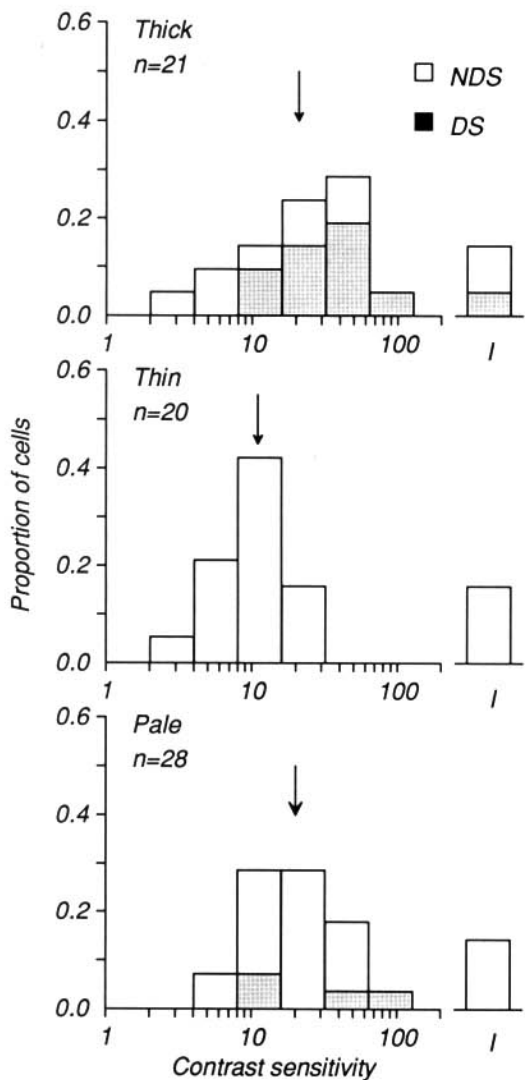


FIG. 14. Distribution of contrast sensitivity of cells in different CO compartments in V2. Directional cells (DS), □ (no contrast data were obtained from DS cells in thin stripes); nondirectional cells, □. Geometric means are indicated (↓; thick, 20.9; thin, 10.9; pale, 20.0).

ties across V2, but here we also indicate the laminar location of cells with particular properties. In this figure, the size of each dot represents the relative incidence of a particular attribute in a particular compartment. A dot that fills the box indicates that all cells in that compartment displayed the attribute; an empty box indicates that no cells displayed the attribute. Only three cells were mapped that could be unequivocally localized to the supragranular layers of a thick stripe, so these boxes have been marked by diagonal lines. (We recorded very few DS cells in the upper layers, even when we include the larger sample in which CO localization was not available. We therefore feel confident in localizing DS cells to the middle layers, in layer 4 or at the 3/4 border, of thick stripes.) In addition, we should note that we did not record equal numbers of cells in each compartment plotted here. This figure shows that whereas these properties were encountered in *all* laminae, color cells were the largest proportion of the population in the upper layers of thin and pale stripes, directional cells in the middle layers

of thick stripes, end-stopped cells in deep layers of thin stripes, and unoriented cells in the middle layers of thin stripes.

DISCUSSION

This study provided a comprehensive set of measurements of the response properties of single neurons in the second visual area, V2, of macaque cerebral cortex, and related those properties to the architecture of V2. We used sinusoidal grating stimuli, which permit a rapid and efficient characterization of receptive fields, and provide a set of measurements readily comparable with those made in other visual areas. It has been suggested that grating stimuli are not appropriate in V2, as its strongly end-stopped receptive fields might be unresponsive to extended grating targets (Hubel and Livingstone 1990). Our experience suggests this is not the case. We mapped all receptive fields with geometric targets before studying their responses to grat-

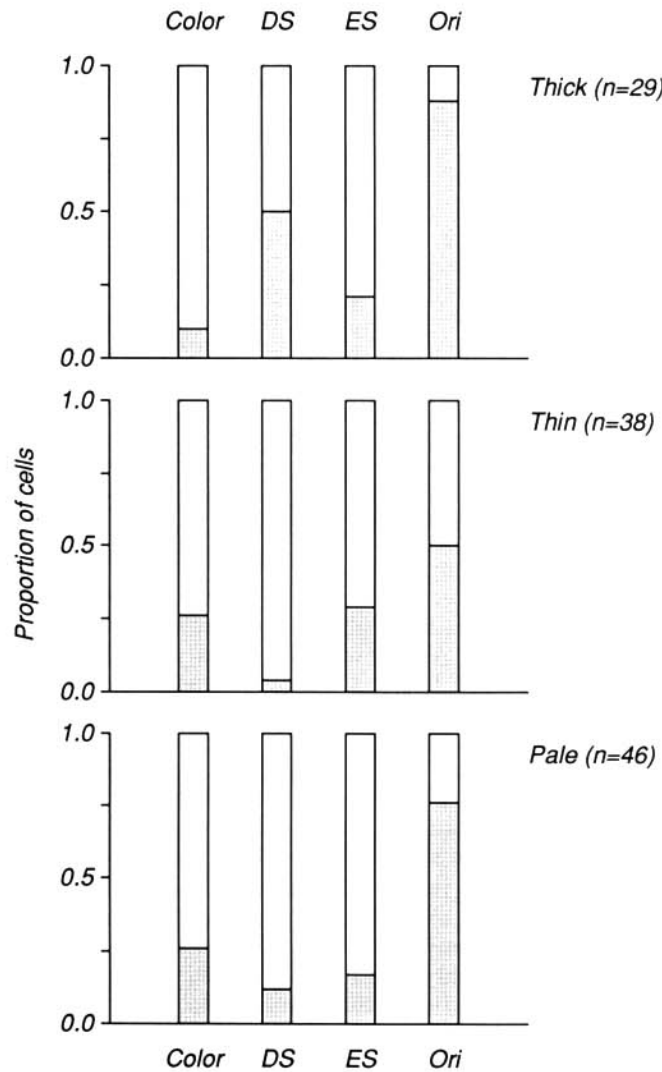


FIG. 15. Relative incidence of properties across V2. Relative frequency (□) of four particular properties in the different CO compartments of V2 are indicated in each histogram. Color, color selectivity; DS, direction selectivity; ES, end stopping; Ori, orientation selectivity. Because these are properties, cells can exhibit >1, and the total in each compartment can therefore sum to >1.

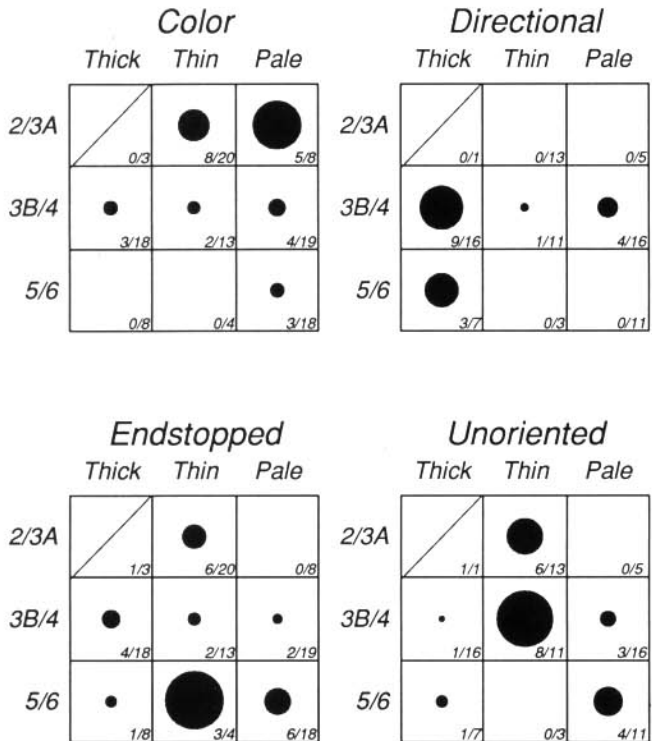


FIG. 16. Plots shown of the same attributes as in Fig. 15; plots also account for the laminar position of the cells. The size of the dot in each box indicates the proportion of cells in that compartment that had that particular selectivity; an empty box indicates that no cells in that compartment exhibited that property. Numbers in the lower right corner of each box indicate the actual numbers of cells measured and positive for that attribute; within any one compartment, cell numbers can vary among attributes because of cells being lost before completing all measurements. For example, unoriented cells comprised a high proportion (8/11) of the middle layers of thin stripes. Only 3 cells were recorded that could be unequivocally localized to the supragranular layers of thick stripes, so those boxes are marked with diagonal lines.

ings. We found few strongly end-stopped cells in V2; and most cells in V2 were driven as well by gratings as by geometric targets. We do not think it likely that we overlooked a significant number of cells: our proportion of unresponsive cells (9%), found in all CO compartments and layers, was very close to that in the awake behaving monkey (11%) (Baizer et al. 1977).

Comparison of V2 properties with other visual areas

ORIENTATION AND DIRECTION SELECTIVITY. In agreement with others, we found that most cells in V2 were orientation selective, although a substantial minority (28%) was unoriented. Previous estimates of the proportion of unoriented cells in V2 have ranged from 16% (Orban et al. 1986) to 27% (Baizer et al. 1977; Zeki 1978). Those cells that were oriented had orientation half-widths ranging from 13° to >90°, with a median value of 28.8°. This agrees well with Baizer et al.'s report (1977) that the modal range of effective orientations in V2 is ~60°. This value is also very similar to the orientation half-widths seen in V4 (26°) (Desimone and Schein 1987), and in MT (34° and 32°) (Gizzi 1983; Albright 1984, respectively), although perhaps somewhat broader than the value of 15–20° observed in V1 (DeValois et al. 1982b). Though different areas may contain

different proportions of oriented or unoriented cells, the oriented cells in each area do not seem to differ markedly in their selectivity. In agreement with previous work (Burkhalter and Van Essen 1986; DeYoe and Van Essen 1985; Orban et al. 1986; Zeki 1978), we also found the relative incidence of direction selectivity in V2 to be low, ~15%. Foster et al. (1985) quote a somewhat higher figure for V2 (38%), although this may simply reflect their less-stringent criterion. In MT, ≥90% of the cells are direction selective (Maunsell and Van Essen 1983a; Zeki 1978), whereas in V4, the proportion is close to that in V2 (Desimone and Schein 1987). As a group, directional cells in V2 had high contrast sensitivities, whether or not they were located in a thick stripe.

Spatial Frequency. Spatial-frequency tuning and selectivity in V2 also differed little from that seen in V1, V4, or MT. The V2 cells' spatial-frequency optima ranged from <0.1 cycles/° up to 7 cycles/°, with a geometric mean of 1.4 cycles/°. We were surprised to find cells that responded well to modulation of a uniform field; V2 receives almost all of its excitatory drive from V1, and few V1 cells respond to full-field flicker (DeValois et al. 1982a; Foster et al. 1985). However, these cells resemble the "luxotonic" units in macaque V1 described by Kayama et al. (1979), and similar cells are observed in V4, a major target of V2 (Desimone and Schein 1987). The cells that responded best to full-field flicker were almost all unoriented and constituted about half of the spatially low-pass group. The range and distribution of spatial-frequency tuning is almost exactly the same as that seen in V4 (Desimone and Schein 1987) and in MT (Gizzi 1983). These values are somewhat lower than what is observed in V1, where optimal spatial frequency can range up to 15 cycles/° or more, and the mean optimal spatial frequency is in the range of 3–4 cycles/° (DeValois et al. 1982a; Foster et al. 1985). Thus whereas the neuronal convergence and receptive-field size increase between V1 and V2 is accompanied by a loss in spatial resolution, there seems to be no such loss in the convergence between V2 and its targets, V4 and MT. There seem to be differences in spatial-frequency bandwidth among these areas. V1 and MT exhibit sharper tuning; mean spatial bandwidths are 1.5–1.8 octaves (DeValois et al. 1982a; Gizzi 1983), whereas the tuning in V2 is somewhat broader (2.4 octaves) and thus more like V4 (2.2 octaves) (Desimone and Schein 1987). One theory concerning V1's role in visual processing is that it acts as a spatial-frequency analyzer. The existence of different sets of neurons selectively responsive to different limited ranges of spatial frequency has led to the suggestion that the visual system, at least through striate cortex, may be doing a spatial-frequency filtering of visual information. Although this role has been suggested for V1, the broader spatial tuning of V2 cells makes it less likely that they are performing a similar frequency-specific analysis. Furthermore if cortical neurons are in fact partitioning the two-dimensional Fourier spectrum, then there might be a relation between the spatial and orientation tuning of neurons. In V1, DeValois et al. (1982a) found a statistically significant positive correlation between spatial-frequency bandwidth and orientation bandwidth. In our V2 sample, we found no correlation be-

tween spatial bandwidth and orientation half-width, another difference with V1.

The only previous report concerning the spatial-frequency tuning of V2 neurons in the macaque is that of Foster et al. (1985), and there were discrepancies between their results and our own. Foster et al. reported that V2 spatial-frequency optima measured at parafoveal eccentricities of 2–5° ranged no higher than 2 cycles/°, with a mean value of 0.65 cycles/°. This is substantially lower than our mean value measured at the same eccentricity range (1.4 cycles/°). Foster et al. also found that spatial bandwidths in V2 were not particularly broad (1.6–1.8 octaves). These values are more like V1, whereas we found spatial bandwidths to be substantially broader in V2 (2.4 octaves). Although we agree that a substantial proportion of V2 cells prefers very low (<0.25 cycles/°) spatial frequencies, their conclusion that the V2 population as a whole is tuned to low frequencies is not in agreement with our data. Perhaps these differences reflect the different anesthetics used in their study (barbiturate) and our own (opiate).

TEMPORAL FREQUENCY. Foster et al. (1985) also examined the temporal properties of V2 neurons, and although most of our data are consistent with theirs, we find certain differences. In agreement with their report, we found that between 35 and 40% of the V2 population is low-pass for temporal frequency, and that V2 cells tend to be most sensitive to drift rates between 3 and 4 Hz. However, they reported that most V2 cells' 50% temporal cutoffs (the high temporal frequency at which responses fell to half the peak value) were 6–12 Hz, with a median value <8 Hz. The median 50% cutoff of our sample was somewhat higher, ~12 Hz. They also showed almost all V2 units having bandwidths <2.5 octaves (mean of 2.1 octaves), whereas we found many units that clearly were much more broadly tuned bandwidths >3–4 octaves (mean of 3.2 octaves).

CORRELATION BETWEEN SPATIAL AND TEMPORAL MEASURES. We performed another set of experiments to examine the relationship between neurons' spatial and temporal tuning. We measured responses to gratings of various spatial frequencies over a range of drift rates and determined whether responses were consistent with spatiotemporal independence as is seen in V1 (Tolhurst and Movshon 1975) or with one form of interaction between these measures: speed tuning. The conclusion drawn from these data is that V2 responses are generally much better correlated with spatiotemporal independence than with this particular prediction for interaction. V2 neurons therefore resemble those in V1; this supports the findings of Foster et al. (1985), who also concluded that spatial and temporal tuning were separable in V2. However, spatial and temporal tuning are not always strictly independent in V2 cells and there is not always an absence of interactions. Some cells' response surfaces showed a clear tilt in this space, indicating some inseparability between spatial and temporal properties, although none specifically matched the velocity prediction. Furthermore as Shapley et al. (1991) have shown, measurement of the spatiotemporal frequency response to gratings drifting in one direction is not a complete test for spatiotemporal independence; a full characterization of the spatiotemporal character of V2 neurons was beyond the scope of this study.

We subjected 12 directional cells to this analysis, and these units seemed essentially the same as nondirectional cells. For some neurons in MT, the spatiotemporal tuning seems nonseparable; the optimal spatial frequency varies with temporal frequency to maintain a constant optimal speed for all stimulus configurations (Movshon et al. 1988). This is a different form of speed tuning than that seen in V1, where the cutoff speed to which a cell will respond varies with the spatial frequency of the stimulus. Speed tuning in this case results from the separate and independent limits placed on response by the spatial and temporal tuning of the cell. The results of this study suggest that the speed tuning observed in V2 neurons (Burkhalter and Van Essen 1986; Orban et al. 1986) arises from a similar mechanism to that in V1. This implies that the speed specificity seen in some units in MT results from processing intrinsic to MT, rather than from specialized inputs from V1 or V2, as none of the V1 or V2 directional units that project to MT seem to be speed tuned in the specific sense we tested here.

CONTRAST. The V2 cells' contrast sensitivities ranged from ~3 up to 100, which corresponds to threshold contrasts from ~0.01 for the most sensitive cells to 0.33 for the least sensitive. The geometric mean threshold contrast was 0.06. It is difficult to make direct comparisons of these figures with others' measurements of contrast sensitivity, as the choice of criterion varies a great deal from group to group. Tolhurst et al. (1983) used the identical technique to define contrast sensitivity in macaque V1, although with a somewhat different threshold criterion, and they found contrast thresholds ranging from 0.02 up to ~0.30 with the mean ~0.08. Therefore our sensitivity values are somewhat inflated relative to theirs, and the contrast sensitivity of V2 cells thus seems to be only slightly higher than that of V1 cells. It is perhaps more convenient to make comparisons using the derived semisaturations and slope parameters of our sample. The median semisaturation contrast was 0.21, and the median value for the exponent governing the steepness of the response function was 2.65. These values mesh nicely with the data of Sclar et al. (1990). They measured these parameters in LGN, V1, and MT and found that at successive stages in the visual pathway, neurons became on average more sensitive to contrast—semisaturations decreased and the steepness of the contrast-response function increased. They showed that a major reason for the change in sensitivity was the increasing size of receptive fields, suggesting that the summation of inputs in larger receptive fields could account for some of the sensitivity increases. In V1, median semisaturation was 0.33, and in MT, 0.07. V2, whose field sizes are larger than V1 but smaller than MT, had a median semisaturation intermediate between these two areas—0.21. The slope parameters also increase in higher areas, indicating steeper response functions. In V1, the median exponent was 2.4, in MT it was 3.0, and we find the value in V2 to be 2.65.

COLOR. Previous estimates of the frequency of color selectivity in V2 have ranged from 16% (Baizer et al. 1977) to 64% (Burkhalter and Van Essen 1986). Based on hand mapping of receptive fields, we classified ~25% of the neurons as color selective. However, these differences are

clearly because of differences in classification criteria. Schein and Desimone (1990) also have shown how criterion shifts affect classification in area V4. We therefore also made quantitative measurements of the color properties of a set of 50 V2 cells. Because similar measurements also have been obtained recently in macaque V1 (Lennie et al. 1990), we compared chromatic properties in V1 and V2.

We found reasonable agreement between our two measures; we classified ~25% of our sample color selective by hand mapping, and 29% of the cells from which we obtained quantitative data had optimal elevations within 45° of the isoluminant plane in our test color space. We found that most cells responded better to modulation of the luminance of a stimulus than to isoluminant color modulations. Although we found some V2 cells with some chromatic opponency (i.e., they responded well to isoluminant color variations), few had *pronounced* opponency. We found no cells that responded exclusively to isoluminant color variations; every cell that responded well to isoluminant color variations responded at least as well to modulations in another plane of color space. Furthermore the distribution of optimal elevations of V2 cells out of the isoluminant plane seemed continuous from 0 to 90°, as was the distribution of ϕ_m s. This result is perhaps not surprising, given that V1 neurons, which provide the major drive to V2 neurons, behave similarly (Lennie et al. 1990). This result is also consistent with the results of Schein and Desimone (1990), who showed little overt color opponency in V4, a major target of V2. That some V2 cells *do* receive chromatically opponent inputs is supported by our finding that the characteristic elevation of some V2 cells dropped when uniform field stimuli were used. Our interpretation is that changing the spatial frequency of stimuli altered the balance between the spatially coextensive chromatically opponent mechanisms driving the V2 cell, and therefore altered its chromatic signature. Flitcroft (1989) has examined the effects of uncorrected chromatic aberration on model neurons and has shown that such effects are significant only for neurons that receive S cone input, and at spatial frequencies >2 cycles/°. Because almost all chromatic gratings we used had spatial frequencies <2 cycles/°, we feel secure in not attributing response differences to luminance artifacts.

V2 cells did seem to differ from V1 cells in the tightness of their tuning in color space and in the linearity with which they combined cone signals. In V1, almost all cells' responses are well described by a model that assumes linear combination of cone signals. In V2, however, we found that the linear model was in general a less satisfactory description of the data. V2 cells were often very narrowly tuned in one plane of color space or were equally responsive in all planes. Another difference between our results and previous work concerns the relation between orientation and color selectivities. In both V1 and V2, it has been reported that most color-selective cells are unoriented (Hubel and Livingstone 1987; Lennie et al. 1990; Livingstone and Hubel 1984). Whereas about half of our color-selective sample was unoriented, we found a number of orientation-selective cells responsive to chromatic modulation. This result is also consistent with Schein and Desimone's (1990) report that these two selectivities seemed unrelated in V4.

Distribution of response properties across V2

In describing the distribution of neuronal properties across V2, it is first necessary to be confident that we could localize accurately recording sites to particular CO stripes. We addressed this issue in METHODS, but we briefly return to it again. We restricted our localization analysis to those penetrations in which we obtained robust CO staining. CO stripes are seen most clearly in tangentially sectioned material, but we chose to section coronally to facilitate laminar assignments. In single coronal sections, CO staining was often variable or ambiguous, so we reconstructed electrode penetrations as well as the local CO stripe pattern from serial sections. Whereas stripe appearance alone often did not suffice to distinguish stripes (even in well-stained material), it was clear that qualitatively different selectivities could be found clustered in (though not restricted to) different stripes (see Figs. 10 and 11), and this often assisted stripe identifications. In a few cases, to obtain a more objective stripe marker, we counterstained sections for Cat-301 to distinguish the thin and thick stripes. Cat-301 cells were clearly distinguishable from CO cells on the basis of the cellular staining pattern, and although the absolute number of labeled cells was low (because of tissue damage sustained during the multiday recording experiment or our conservative counting criteria of using only the most intensely stained cells), our different methods of identifying stripes always matched. We are therefore confident that we have accurately distinguished the different CO compartments.

We found striking similarities in response characteristics of cells in the different CO stripes, despite the qualitative differences of some cells within them. In agreement with previous reports (DeYoe and Van Essen 1985; Hubel and Livingstone 1985, 1987), we found that directional cells are found clustered more frequently in different stripes. However, in agreement with DeYoe and Van Essen (1985), we found that cells with any attribute could be found in any compartment, though clustered or more numerous only in the "appropriate" compartment. Peterhans and von der Heydt (1993) recently came to the same conclusion in the alert macaque, although they found direction-selective neurons more evenly distributed across V2 than we did.

There are also discrepancies between our data and previous reports on the localization of certain types of cells. Hubel and Livingstone (1987) reported that cells in the thin stripes were nearly all unoriented, many were color coded and that end-stopped cells were especially prominent in the pale stripes. They also reported that very few oriented cells showed overt color coding. We found end-stopped cells primarily in both pale and thin stripes. Whereas unoriented cells certainly most likely were to be found in thin stripes, we found that only about a half of the cells in these stripes were unoriented. We found that cells classified as color selective were equally likely to be oriented or unoriented. As noted above, the root of this discrepancy might be how cells were classified as color selective, or might reflect a species difference between the squirrel monkeys used in most of their recordings and the macaques used in ours.

Earlier reports also emphasized the distributions of cells with special selectivities. We were surprised to find that a prominent cell group in all stripe compartments was a va-

nilla cell: a nonend-stopped oriented complex cell with no color or direction selectivity. Hubel and Livingstone (1987) defined a similar class, and called these cells oriented complex. They noted in their 1987 paper that this group was "a very prominent group of cells in area 18". Baizer et al. (1977) also describe this group (orientation cells) as the most common V2 cell class.

One stimulus selectivity that is reported to be important in V2 is that for binocular disparity. Hubel and Wiesel (1970) and Poggio and Fischer (1977) demonstrated that many cells in V2 are sensitive to binocular disparity, and Hubel and Livingstone (1987) reported that disparity-sensitive cells are restricted to the thick stripes, although Petersen and von der Heydt (1993) found such cells in all compartments. We did not test disparity sensitivity, and it is possible that a few cells we classified as vanilla or unresponsive were either obligate binocular or were cells to which we simply did not present the optimal stimulus. However, the fact that such cells were found roughly uniformly in *all* CO compartments suggests that we were not systematically overlooking cells with any particular selectivity.

QUANTITATIVE RESPONSE DIFFERENCES AND P/M SEGREGATION. We found distinctive differences in the localization of particular cell types, yet the most striking feature of V2 organization was its homogeneity. We found few quantitative differences among cells in different compartments. If these different domains really do derive their predominant excitatory drive from either P or M signals, then one might expect to find related response differences between different stripe domains. Cells in thin or pale stripes, nominally driven by P signals, should prefer higher spatial and lower temporal frequencies and have lower contrast sensitivities. Conversely thick stripes, nominally dominated by M input, should contain cells with higher contrast sensitivity and that are tuned to lower spatial and higher temporal frequencies. It must be understood, however, that the responses of V2 cells need not simply reflect the characteristics of P or M cells. For example, contrast sensitivity may not be a reliable indication of the type of input to a neuron. High sensitivities could result as easily from neural convergence of parvocellular signals as from magnocellular input; V1 and V2 cells may well be more sensitive than their parvocellular afferents simply because of the summation of inputs in their larger receptive fields.

With this limitation in mind, our data indicate that there is much less segregation of P and M signals in V2 than might have been expected. Optimal spatial frequency, optimal temporal frequency, temporal resolution, spatial bandwidth, and temporal bandwidth in different compartments were all indistinguishable. Nor was there any particular relationship between the spatial and temporal tuning of neurons in any stripe region. There were small and statistically insignificant differences in spatial resolution among the stripes; thick and pale stripes both had higher resolution than thin stripes, and were indistinguishable from one another. Tootell and Hamilton (1989) found using 2DG labelling, that low-spatial-frequency stimuli labeled thick and thin stripes more than pale stripes, whereas high-spatial-frequency stimuli preferentially labeled columns of cells that seemed to coincide with the pale stripes. These apparent

differences may be related to the distribution of low-pass cells in the different compartments, which would contribute heavily to 2DG patterns. Tootell and Hamilton also found that spatially diffuse color variations selectively labeled thin stripes, but spatially diffuse luminance changes produced no uptake in V2. Here we are in better agreement with the 2DG results. Our data indicate that V2 contains some cells that are low-pass for spatial frequency and respond well to spatially uniform modulations. These cells were almost all unoriented, and located in thin stripes. Some of these unoriented cells responded well to modulations of stimulus chromaticity and could be the cells responsible for the increased uptake in response to spatially diffuse color variations. However, some of these cells clearly responded well to spatially diffuse luminance modulation as well. Perhaps their numbers are too small to cause a detectable increase in 2DG uptake, and for that reason they were not detected by Tootell and Hamilton. The existence of these cells in thin stripes is consistent with the known anatomy and physiology of the V1 cytochrome oxidase-blob regions. Cells in V1 blobs are often color sensitive, unoriented, and prefer low spatial frequencies (Born and Tootell 1991; Silverman et al. 1989), and it is the V1 blobs that project to the V2 thin stripes (Livingstone and Hubel 1984).

There were also significant differences in contrast sensitivity, but the differences were not precisely the ones expected. As anticipated, thick-stripe cells were among the most sensitive. This is consistent with their receiving a dominant M input and with Tootell and Hamilton's (1989) report that in V2, low-contrast stimuli seemed to label only every other stripe, which they took to be the thick stripes. It is noteworthy, though, that only the directional cells in the thick stripes were sensitive. Other cells within thick stripes were no more sensitive than cells in other compartments. Thin-stripe cells were substantially less sensitive, consistent with their claimed P inputs. However, we also inconveniently found that pale-stripe cells were as sensitive as thick-stripe cells. As noted above, this does not necessarily imply M input to the pale stripes. Indeed Hubel and Livingstone (1990) showed that cells in the top layers of V1 (including those in the layer 2/3 interblobs, which project to the pale stripes) can be as sensitive as cells in layers 4B and 4C α . This also agrees with Tootell et al. (1988), who showed that stimulating V1 with low-contrast stimuli elicited some labeling in the top layers, which are the layers providing input to the thin and pale stripes.

In retrospect, the lack of segregation we observe should not be surprising, because it is becoming clear that there is no strict segregation of these signals in the cortex. Anatomic studies in V1 have long recognized links from layers 4C α and 4B to the top layers (Blasdel et al. 1985; Fitzpatrick et al. 1985; Lund and Boothe 1975), and recent studies have demonstrated explicitly the P/M convergence in both blob and interblob compartments (Lachica et al. 1992; Yoshioka et al. 1994). This convergence of P and M signals in the upper layers of V1, suggested by the anatomy, has been demonstrated physiologically by studies that selectively inactivated P or M divisions of the LGN; these studies showed that many V1 units receive excitatory drive from *both* parvocellular and magnocellular laminae (Malpeli et

al. 1981) and that there is a rich M input to the upper layers of V1 as well as to V4 (Nealey et al. 1991). What is surprising, therefore, about our contrast-sensitivity results is not that pale-stripe cells are as sensitive as thick-stripe cells, but rather that thin-stripe cells are so relatively *insensitive*. In V2 itself, another possible mechanism for P/M convergence could be the back projections from V4 and MT. Although distinct V2 subregions provide ascending outputs to these areas, it seems that the feedback connections to V2 terminate less specifically, over all stripe divisions (Krubitzer and Kaas 1989; Shipp and Zeki 1989b; Zeki and Shipp 1989). Local connectivity within V2 also provides a substrate for signal convergence; unlike stripe domains are prominently interconnected (Levitt et al. 1994; Livingstone and Hubel 1984). The relative homogeneity of many neuronal response properties within V2 presumably reflects this massive anatomic convergence.

COMPARISON OF COLOR-AND DIRECTION-SELECTIVE CELLS IN v2. We were concerned that our inability to localize all neurons histologically might have obscured important aspects of their organization. We therefore made another kind of analysis, in which we compared the properties of cells with qualitatively different *attributes*, without regard to their location.

We know that the different stripe regions of V2 have different extrinsic anatomic projections and that the qualitative properties of some cells within these stripes match the properties of cells in their target areas (e.g., color-selective cells in thin and pale stripes that project to V4, and direction-selective cells in thick stripes that project to MT). However, many cells in each stripe region show no particular selectivity. The distinctive cells are generally a *minority* of the population within each stripe. We wished to compare directly those cells that confer on each stripe region its distinctive character and that are presumably responsible for the differences seen between streams of visual information through cortex. For these reasons, we chose to compare the response properties of color-selective cells versus directional cells. These types seem clearly differentially distributed across V2 and are most likely to be related to different processing streams.

There were no significant differences in the spatial or temporal properties of these groups, although the color-selective group was distinguished by containing some cells that responded well to full-field flicker and were temporally low-pass. The only parameter that reliably differentiated these two groups was contrast sensitivity. The mean contrast sensitivity of directional cells was more than double that of color cells, 28.3 versus 13.3, and this difference was significant ($U = 84.5$, $z = 2.24$, $P < 0.03$). This is the only one of our response measures that robustly supports the notion of a segregation of P and M signals through V2.

These two classes of cells also were distinguished by their laminar distribution. Color cells, though found in all laminae, were found predominantly in the supragranular layers 2 and top 3. This was supported by our quantitative measurements of color properties. Directional cells had a complementary laminar distribution; most were found in layers 3B or 4. These findings are consistent with the anatomy of V2's projections to higher cortical areas, particularly V4

and MT, which are among V2's major ascending cortical targets. The projection to area MT arises from those layers where the directional cells are most common (Lund et al. 1981; Shipp and Zeki 1989b). Color cells are prominent in the upper layers, which are the source of the projection to area V4 (Zeki and Shipp 1989). Recently, Peterhans and von der Heydt (1993) described less-distinct laminar segregation of functional characteristics; this may relate to differences in cell classification or to histological inaccuracies in their chronic recording preparation. Although we acknowledge this disagreement in the dependence of functional properties on laminar position, our data suggest that an important determinant of a V2 neuron's properties may be whether or not it sits in a layer containing projection neurons to higher areas.

MODULARITY WITHIN v2. It also became clear during these recordings that response properties varied even within a single compartment. When traversing a stripe, we often encountered a cluster of cells having similar properties and then recorded from cells having different characteristics. For example, in thin stripes, we often recorded a run of several consecutive unoriented cells, which then were followed by several vanilla cells. There is already evidence for such substructure within the stripes. Anatomic studies of the projection from V2 to V4 and MT have shown that the cells in the thick stripes that project to MT, and the cells in the thin and pale stripes that project to V4, are not continuously distributed through each stripe, but rather as discrete clusters within each stripe (DeYoe and Van Essen 1985; Shipp and Zeki 1989b; Zeki and Shipp 1989). This anatomic substructure in the stripes also has been seen in other studies of V2. Tootell and Hamilton (1989) showed in their 2DG study of V2 that in many cases the pattern of 2DG uptake within a stripe was not continuous but patchy. This finding agrees nicely with other studies showing that local connectivity *within* stripes is also patchy (Levitt et al. 1994). The stripes therefore seem more like collections of beads or patches than continuous domains. The clustering of cells with similar properties may reveal a physiological substructure mirroring the anatomic one.

V2 RECEPTIVE FIELDS AND FUNCTIONAL SEGREGATION. We have presented evidence that V2 is in many respects similar to its major input, V1, and to two of its major cortical outputs, V4 and MT. Is there any suggestion of what V2's role in visual processing might be? The anatomy of V2 suggests some possibilities. In V2, although inputs and outputs are segregated, regions that relay different types of visual information are arranged into adjacent parallel stripes of tissue. Given the laterally spreading connections that have already been described within V2 (Levitt et al. 1994; Livingstone and Hubel 1984; Lund et al. 1981; Rockland 1985), it seems that V2 is a place where much interaction might occur between different channels of visual information. The functional similarities we observe among neurons in different CO stripes may reflect this interaction. There is also evidence from physiological studies showing that V2 neurons do exhibit properties not seen earlier in the visual pathway. Von der Heydt and Peterhans (1989) have shown that V2 neurons respond to illusory contour stimuli, a property that is not seen in V1 neurons. Our data on the color proper-

ties of V2 neurons suggest that these cells may be combining cone signals differently than has been seen in the LGN and striate cortex. Clearly V2 does more than simply relay visual information from V1 to higher visual centers.

Our data provide only equivocal support for the idea that the CO compartments in V2 capture the continued segregation of parallel functional pathways in the visual cortex. Although qualitatively different groups of cells do seem to cluster into different stripe compartments (and have a restricted laminar localization within each compartment), this segregation is not absolute, and the quantitative differences in response properties among compartments are rather subtle. Moreover, a very common cell type in all compartments is the vanilla cell, which lacks the distinctive properties suggested to distinguish the different pathways. Thus one can choose to emphasize either the differences or the similarities among different stripe compartments in V2. Although previous studies of V2 have emphasized the differences between V2 compartments, our results suggest a strong commonality of neuronal properties across all the divisions of this pivotal visual area. It would certainly be a mistake to view V2 as a set of purely segregated waystations for a set of parallel pathways that wend their independent ways further into the extrastriate visual cortex.

We thank S. Fenstermaker for assisting with histology and in some of the recordings, J. Krauskopf for help subduing the Adage display processor, and S. Hockfield for making the Cat-301 antibody available to us. J. Maunsell provided helpful comments on an earlier version of the manuscript.

This work was supported by a National Institute of Mental Health predoctoral fellowship to J. B. Levitt (MH-09692), by a Young Scientist Fellowship from the Fonds National Suisse pour la Recherche to D. C. Kiper, and by National Institutes of Health Grants EY-02017 (to J. A. Movshon) and EY-05864 (to L. Kiorpes).

Present address: J. B. Levitt, Dept. of Visual Science, Institute of Ophthalmology, 11–43 Bath St., London EC1V 9EL, England; D. C. Kiper, Institut d'anatomie, Faculté de médecine, Université de Lausanne, Rue du Bugnon 9, 1005 Lausanne, Switzerland.

Address for reprint requests: J. A. Movshon, Center for Neural Science, New York University, 4 Washington Place, Room 809, New York, NY 10003.

Received 18 August 1993; accepted in final form 21 January 1994.

REFERENCES

- ALBRECHT, D. G. AND HAMILTON, D. B. Striate cortex of monkey and cat: contrast response function. *J. Neurophysiol.* 48: 217–237, 1982.
- ALBRIGHT, T. D. Direction and orientation selectivity of neurons in visual area MT of the macaque. *J. Neurophysiol.* 52: 1106–1130, 1984.
- BAIZER, J. S., ROBINSON, D. L., AND DOW, B. M. Visual responses of area 18 neurons in awake, behaving monkey. *J. Neurophysiol.* 40: 1024–1037, 1977.
- BLASDEL, G. G., LUND, J. S., AND FITZPATRICK, D. Intrinsic connections of macaque striate cortex: axonal projections of cells outside lamina 4C. *J. Neurosci.* 5: 3350–3369, 1985.
- BORN, R. T. AND TOOTELL, R. B. H. Spatial frequency tuning of single units in macaque supragranular striate cortex. *Proc. Natl. Acad. Sci. USA* 88: 7066–7070, 1991.
- BURKHALTER, A. AND VAN ESSEN, D. C. Processing of color, form, and disparity information in visual areas VP and V2 of ventral extrastriate cortex in the macaque monkey. *J. Neurosci.* 6: 2327–2351, 1986.
- DERRINGTON, A. M., KRAUSKOPF, J., AND LENNIE, P. Chromatic mechanisms in lateral geniculate nucleus of macaque. *J. Physiol. Lond.* 357: 241–265, 1984.
- DERRINGTON, A. M. AND LENNIE, P. Spatial and temporal contrast sensitivity of neurones in lateral geniculate nucleus of macaque. *J. Physiol. Lond.* 357: 219–240, 1984.
- DESIMONE, R. AND SCHEIN, S. J. Visual properties of neurons in area V4 of the macaque: sensitivity to stimulus form. *J. Neurophysiol.* 57: 835–868, 1987.
- DESIMONE, R., SCHEIN, S. J., MORAN, J., AND UNGERLEIDER, L. G. Contour, color, and shape analysis beyond the striate cortex. *Vision Res.* 25: 441–452, 1985.
- DEVALOIS, R. L., ALBRECHT, D. G., AND THORELL, L. G. Spatial frequency selectivity of cells in macaque visual cortex. *Vision Res.* 22: 545–559, 1982a.
- DEVALOIS, R. L., YUND, E. W., AND HEPLER, N. The orientation and direction selectivity of cells in macaque visual cortex. *Vision Res.* 22: 531–544, 1982b.
- DEYOE, E. A., HOCKFIELD, S., GARREN, H., AND VAN ESSEN, D. C. Antibody labeling of functional subdivisions in visual cortex: Cat-301 immunoreactivity in striate and extrastriate cortex of the macaque monkey. *Visual Neurosci.* 5: 67–81, 1990.
- DEYOE, E. A. AND VAN ESSEN, D. C. Segregation of efferent connections and receptive field properties in visual area V2 of the macaque. *Nature Lond.* 317: 58–61, 1985.
- DEYOE, E. A. AND VAN ESSEN, D. C. Concurrent processing streams in monkey visual cortex. *Trends Neurosci.* 11: 219–226, 1988.
- DREHER, B., FUKADA, Y., AND RODECK, R. W. Identification, classification, and anatomic segregation of cells with X-like and Y-like properties in the lateral geniculate nucleus of Old World primates. *J. Physiol. Lond.* 258: 433–452, 1976.
- DUBNER, R. AND ZEKI, S. M. Response properties and receptive fields of cells in an anatomically defined region of the superior temporal sulcus in the monkey. *Brain Res.* 35: 528–532, 1971.
- FELLEMAN, D. J. AND VAN ESSEN, D. C. Distributed hierarchical processing in the primate cerebral cortex. *Cereb. Cortex* 1: 1–47, 1991.
- FITZPATRICK, D., LUND, J. S., AND BLASDEL, G. G. Intrinsic connections of macaque striate cortex: afferent and efferent connections of lamina 4C. *J. Neurosci.* 5: 3329–3349, 1985.
- FLITCROFT, D. I. The interactions between chromatic aberration, defocus, and stimulus chromaticity: implications for visual physiology and colorimetry. *Vision Res.* 29: 349–360, 1989.
- FOSTER, K. H., GASKA, J. P., NAGLER, M., AND POLLEN, D. A. Spatial and temporal frequency selectivity of neurons in visual cortical areas V1 and V2 of the macaque monkey. *J. Physiol. Lond.* 365: 331–363, 1985.
- GATTASS, R., GROSS, C. G., AND SANDELL, J. H. Visual topography of V2 in the macaque. *J. Comp. Neurol.* 201: 519–539, 1981.
- GEGENFURTNER, K. G., KIPER, D. C., AND FENSTERMAKER, S. B. Chromatic properties of neurons in macaque V2. *Soc. Neurosci. Abstr.* 19: 769, 1993.
- GIZZI, M. S. *The processing of visual motion in cat and monkey central nervous system*. (PhD dissertation). New York: New York University, 1983.
- HAWKEN, M. J., PARKER, A. J., AND LUND, J. S. Laminar organization and contrast sensitivity of direction-selective cells in the striate cortex of the Old World monkey. *J. Neurosci.* 8: 3541–3548, 1988.
- HENDRICKSON, A. E., WILSON, J. R., AND OGREN, M. P. The neuroanatomic organization of pathways between the dorsal lateral geniculate nucleus and visual cortex in Old World and New World primates. *J. Comp. Neurol.* 182: 123–136, 1978.
- HENDRY, S. H. C., JONES, E. G., HOCKFIELD, S., AND MACKAY, R. D. G. Neuronal populations stained with the monoclonal antibody Cat-301 in the mammalian cerebral cortex and thalamus. *J. Neurosci.* 9: 2432–2442, 1988.
- HICKS, T. P., LEE, B. B., AND VIDYASAGAR, T. R. The responses of cells in macaque lateral geniculate nucleus to sinusoidal gratings. *J. Physiol. Lond.* 337: 183–200, 1983.
- HORTON, J. C. AND HUBEL, D. H. Regular patchy distribution of cytochrome oxidase staining in primary visual cortex of macaque monkey. *Nature Lond.* 292: 762–764, 1981.
- HUBEL, D. H. AND LIVINGSTONE, M. S. Complex-unoriented cells in a subregion of primate area 18. *Nature Lond.* 315: 325–327, 1985.
- HUBEL, D. H. AND LIVINGSTONE, M. S. Segregation of form, color, and stereopsis in primate area 18. *J. Neurosci.* 7: 3378–3415, 1987.
- HUBEL, D. H. AND LIVINGSTONE, M. S. Color and contrast sensitivity in the lateral geniculate body and primary visual cortex of the macaque monkey. *J. Neurosci.* 10: 2223–2237, 1990.
- HUBEL, D. H. AND WIESEL, T. N. Cells sensitive to binocular depth in area 18 of the macaque monkey cortex. *Nature Lond.* 225: 141–142, 1970.
- HUBEL, D. H. AND WIESEL, T. N. Laminar and columnar distribution of

- geniculocortical fibers in macaque monkey. *J. Comp. Neurol.* 146: 421–450, 1972.
- HUMPHREY, A. L. AND HENDRICKSON, A. E. Background and stimulus-induced patterns of high metabolic activity in the visual cortex (area 17) of the squirrel and macaque monkey. *J. Neurosci.* 3: 345–358, 1983.
- KAPLAN, E. AND SHAPLEY, R. M. X and Y cells in the lateral geniculate nucleus of macaque monkeys. *J. Physiol. Lond.* 330: 125–143, 1982.
- KAYAMA, Y., RISO, R. R., BARTLETT, J. R., AND DOTY, R. W. Luxotonic responses of units in macaque striate cortex. *J. Neurophysiol.* 42: 1495–1517, 1979.
- KRUBITZER, L. A. AND KAAS, J. H. Cortical integration of parallel pathways in the visual system of primates. *Brain Res.* 478: 161–165, 1989.
- LACHICA, E. A., BECK, P. D., AND CASAGRANDE, V. A. Parallel pathways in macaque monkey striate cortex: anatomically defined columns in layer III. *Proc. Natl. Acad. Sci. USA* 89: 3566–3570, 1992.
- LENNIE, P., KRAUSKOPF, J., AND SCLAR, G. Chromatic mechanisms in striate cortex of macaque. *J. Neurosci.* 10: 649–669, 1990.
- LEVITT, J. B., KIPER, D. C., AND MOVSHON, J. A. Distribution of neuronal response properties in macaque V2. *Soc. Neurosci. Abstr.* 16: 293, 1990.
- LEVITT, J. B., YOSHIOKA, T., AND LUND, J. S. Intrinsic cortical connections in macaque visual area V2: evidence for interaction between different functional streams. *J. Comp. Neurol.* 342: 551–570, 1994.
- LIVINGSTONE, M. S. AND HUBEL, D. H. Anatomy and physiology of a color system in the primate visual cortex. *J. Neurosci.* 4: 309–356, 1984.
- LIVINGSTONE, M. S. AND HUBEL, D. H. Connections between layer 4b of area 17 and the thick cytochrome oxidase stripes of area 18 in the squirrel monkey. *J. Neurosci.* 7: 3371–3377, 1987.
- LIVINGSTONE, M. S. AND HUBEL, D. H. Segregation of form, color, movement, and depth: anatomy, physiology, and perception. *Science Wash. DC* 240: 740–749, 1988.
- LUND, J. S. AND BOOTHE, R. G. Interlaminar connections and pyramidal neuron organization in the visual cortex, area 17, of the macaque monkey. *J. Comp. Neurol.* 159: 305–334, 1975.
- LUND, J. S., HENDRICKSON, A. E., OGREN, M. P., AND TOBIN, E. A. Anatomic organization of primate visual cortex area VII. *J. Comp. Neurol.* 202: 19–45, 1981.
- MALPELI, J. G., SCHILLER, P. H., AND COLBY, C. L. Response properties of single cells in monkey striate cortex during reversible inactivation of individual lateral geniculate laminae. *J. Neurophysiol.* 46: 1102–1119, 1981.
- MANSFIELD, R. J. W. Neural basis of orientation perception in primate vision. *Science Wash. DC* 186: 133–135, 1974.
- MAUNSELL, J. H. R., NEALEY, T. A., AND DEPRIEST, D. D. Magnocellular and parvocellular contributions to responses in the middle temporal visual area (MT) of the macaque monkey. *J. Neurosci.* 10: 3323–3334, 1990.
- MAUNSELL, J. H. R. AND NEWSOME, W. T. Visual processing in monkey extrastriate cortex. *Annu. Rev. Neurosci.* 10: 363–401, 1987.
- MAUNSELL, J. H. R. AND VAN ESSEN, D. C. Functional properties of neurons in middle temporal visual area of the macaque monkey. I. Selectivity for stimulus direction, speed, and orientation. *J. Neurophysiol.* 49: 1127–1147, 1983a.
- MAUNSELL, J. H. R. AND VAN ESSEN, D. C. Functional properties of neurons in middle temporal visual area of the macaque monkey. II. Binocular interactions and sensitivity to binocular disparity. *J. Neurophysiol.* 49: 1148–1167, 1983b.
- MERIGAN, W. H., KATZ, L. M., AND MAUNSELL, J. H. R. The effects of parvocellular lateral geniculate lesions on the acuity and contrast sensitivity of macaque monkeys. *J. Neurosci.* 11: 994–1001, 1991.
- MERIGAN, W. H. AND MAUNSELL, J. H. R. Macaque vision after magnocellular lateral geniculate lesions. *Visual Neurosci.* 5: 347–352, 1990.
- MERRILL, E. G. AND AINSWORTH, A. Glass-coated platinum-plated tungsten microelectrode. *Med. Biol. Eng.* 10: 495–504, 1972.
- MOVSHON, J. A., ADELSON, E. H., GIZZI, M. S., AND NEWSOME, W. T. The analysis of moving visual patterns. In: *Pattern Recognition Mechanisms: Pontificiae Academiae Scientiarum Scripta Varia*, edited by C. Chagas, R. Gattass, and C. Gross. Rome: Vatican Press, 1985, vol. 54, p. 117–151.
- MOVSHON, J. A. AND NEWSOME, W. T. Functional characteristics of striate cortical neurons projecting to MT in the macaque. *Soc. Neurosci. Abstr.* 10: 933, 1984.
- MOVSHON, J. A., NEWSOME, W. T., GIZZI, M. S., AND LEVITT, J. B. Spatio-temporal tuning and speed sensitivity in macaque visual cortical neurons. *Invest. Ophthalmol. Visual Sci.* 29, Suppl.: 327, 1988.
- MOVSHON, J. A., THOMPSON, I. D., AND TOLHURST, D. J. Spatial summation in the receptive fields of simple cells in the cat's striate cortex. *J. Physiol. Lond.* 283: 57–77, 1978a.
- MOVSHON, J. A., THOMPSON, I. D., AND TOLHURST, D. J. Receptive-field organization of complex cells in the cat's striate cortex. *J. Physiol. Lond.* 283: 79–99, 1978b.
- NEALEY, T. A., FERRERA, V. P., AND MAUNSELL, J. H. R. Magnocellular and parvocellular contributions to the ventral extrastriate cortical processing stream. *Soc. Neurosci. Abstr.* 17: 525, 1991.
- ORBAN, G. A., KENNEDY, H., AND BULLIER, J. Velocity sensitivity and direction selectivity of neurons in areas V1 and V2 of the monkey: influence of eccentricity. *J. Neurophysiol.* 56: 462–480, 1986.
- PETERHANS, E. AND VON DER HEYDT, R. Mechanisms of contour perception in monkey visual cortex. II. Contours bridging gaps. *J. Neurosci.* 9: 1749–1763, 1989.
- PETERHANS, E. AND VON DER HEYDT, R. Functional organization of area V2 in the alert macaque. *Eur. J. Neurosci.* 5: 509–524, 1993.
- POGGIO, G. F. AND FISCHER, B. Binocular interaction and depth sensitivity in striate and prestriate cortex of behaving rhesus monkey. *J. Neurophysiol.* 40: 1392–1405, 1977.
- ROCKLAND, K. S. A reticular pattern of intrinsic connections in primate area V2 (area 18). *J. Comp. Neurol.* 235: 467–478, 1985.
- SCHEIN, S. J. AND DESIMONE, R. Spectral properties of V4 neurons in the macaque. *J. Neurosci.* 10: 3369–3389, 1990.
- SCHILLER, P. H., LOGOTHETIS, N. K., AND CHARLES, E. R. Functions of the color-opponent and broad-band channels of the visual system. *Nature Lond.* 343: 68–70, 1990.
- SCHILLER, P. H. AND MALPELI, J. G. Functional specificity of lateral geniculate nucleus laminae of the rhesus monkey. *J. Neurophysiol.* 41: 788–797, 1978.
- SCLAR, G., MAUNSELL, J. H. R., AND LENNIE, P. Coding of image contrast in central visual pathways of the macaque monkey. *Vision Res.* 30: 1–10, 1990.
- SHAPLEY, R., REID, R. C., AND SOODAK, R. Spatiotemporal receptive fields and directional selectivity. In: *Computational Models of Visual Processing*, edited by M. S. Landy and J. A. Movshon. Cambridge, MA: MIT Press, 1991, p. 109–118.
- SHERMAN, S. M., SCHUMER, R. A., AND MOVSHON, J. A. Functional cell classes in the macaque's LGN. *Soc. Neurosci. Abstr.* 10: 296, 1984.
- SHIPP, S. AND ZEKI, S. Segregation of pathways leading from area V2 to areas V4 and V5 of macaque monkey visual cortex. *Nature Lond.* 315: 322–325, 1985.
- SHIPP, S. AND ZEKI, S. The organization of connections between areas V5 and V1 in macaque monkey visual cortex. *Eur. J. Neurosci.* 1: 309–332, 1989a.
- SHIPP, S. AND ZEKI, S. The organization of connections between areas V5 and V2 in macaque monkey visual cortex. *Eur. J. Neurosci.* 1: 333–354, 1989b.
- SILVERMAN, M. S., GROSOFF, D. H., DEVALOIS, R. L., AND ELFAR, S. D. Spatial-frequency organization in primate striate cortex. *Proc. Natl. Acad. Sci. USA* 86: 711–715, 1989.
- SILVERMAN, M. S. AND TOOTELL, R. B. H. Modified technique for cytochrome oxidase histochemistry: increased staining intensity and compatibility with 2-deoxyglucose autoradiography. *J. Neurosci. Methods* 19: 1–10, 1987.
- SKOTTUN, B. C., DEVALOIS, R. L., GROSOFF, D. H., MOVSHON, J. A., ALBRECHT, D. G., AND BONDS, A. B. Classifying simple and complex cells on the basis of response modulation. *Vision Res.* 31: 1079–1086, 1991.
- TOLHURST, D. J. AND MOVSHON, J. A. Spatial and temporal contrast sensitivity of striate cortical neurones. *Nature Lond.* 257: 674–675, 1975.
- TOLHURST, D. J., MOVSHON, J. A., AND DEAN, A. F. The statistical reliability of signals in single neurons in cat and monkey visual cortex. *Vision Res.* 23: 775–785, 1983.
- TOOTELL, R. B. H. AND HAMILTON, S. L. Functional anatomy of the second visual area (V2) in the macaque. *J. Neurosci.* 9: 2620–2644, 1989.
- TOOTELL, R. B. H., HAMILTON, S. L., AND SWITKES, E. Functional anatomy of macaque striate cortex. IV. Contrast and magno-parvo streams. *J. Neurosci.* 8: 1594–1609, 1988.
- UNGERLEIDER, L. G. AND MISHKIN, M. Two cortical visual systems. In: *Analysis of Visual Behavior*, edited by D. J. Ingle, M. A. Goodale, and R. J. W. Mansfield. Cambridge, MA: MIT Press, 1982, p. 549–586.
- VAN ESSEN, D. C. Functional organization of primate visual cortex. In: *Cerebral Cortex*, edited by A. Peters and E. G. Jones. New York: Plenum, 1985, vol. 3, p. 259–329.
- VAN ESSEN, D. C., FELLEMAN, D. J., DEYO, E. A., OLAVARRIA, J., AND

- KNIERIM, J. Modular and hierarchical organization of extrastriate visual cortex in the macaque monkey. *Cold Spring Harbor Symp. Quant. Biol.* 55: 679-696, 1990.
- VAN ESSEN, D. C. AND MAUNSELL, J. H. R. Hierarchical organization and functional streams in the visual cortex. *Trends Neurosci.* 6: 370-375, 1983.
- VON DER HEYDT, R. AND PETERHANS, E. Mechanisms of contour perception in monkey visual cortex. I. Lines of pattern discontinuity. *J. Neurosci.* 9: 1731-1748, 1989.
- WIESEL, T. N. AND HUBEL, D. H. Spatial and chromatic interactions in the lateral geniculate body of the rhesus monkey. *J. Neurophysiol.* 29: 1115-1156, 1966.
- WONG-RILEY, M. T. T. Changes in the visual system of monocularly sutured and enucleated cat demonstrated with cytochrome oxidase histochemistry. *Brain Res.* 171: 11-28, 1979.
- YOSHIOKA, T., LEVITT, J. B., AND LUND, J. S. Independence and merger of thalamocortical channels within macaque monkey primary visual cortex: anatomy of interlaminar projections. *Visual Neurosci.* 11: 467-489, 1994.
- ZEKI, S. M. Functional organization of a visual area in the posterior bank of the superior temporal sulcus of the rhesus monkey. *J. Physiol. Lond.* 236: 549-573, 1974.
- ZEKI, S. M. Uniformity and diversity of structure and function in rhesus monkey prestriate visual cortex. *J. Physiol. Lond.* 277: 273-290, 1978.
- ZEKI, S. AND SHIPP, S. Modular connections between areas V2 and V4 of macaque monkey visual cortex. *Eur. J. Neurosci.* 1: 494-506, 1989.